HHS Public Access

Author manuscript

Glia. Author manuscript; available in PMC 2020 June 03.

Published in final edited form as:

Glia. 2020 June ; 68(6): 1165–1181. doi:10.1002/glia.23768.

Schwann cells orchestrate peripheral nerve inflammation through the expression of CSF1, IL-34 and SCF in Amyotrophic Lateral Sclerosis

Emiliano Trias[1], **Mariángeles Kovacs**[1], **Peter H. King**[2,3], **Ying Si**[2,3], **Yuri Kwon**[2], **Valentina Varela**[1], **Sofía Ibarburu**[1], **Ivan C. Moura**[4,5,6,7,8,9,†], **Olivier Hermine**[4,5,6,7,8,9,10,11,12], **Joseph S. Beckman**[13], **Luis Barbeito**[1,j]

[1]Institut Pasteur de Montevideo, Uruguay

[2]Department of Neurology, University of Alabama, Birmingham, AL 35294

[3]Birmingham Veterans Affairs Medical Center, Birmingham, AL 35295

[4]Imagine Institute, Hôpital Necker, Paris, France

[5]INSERM UMR 1163, Laboratory of Cellular and Molecular echanisms of Hematological Disorders and Therapeutic Implications, Paris, France.

[6]Paris Descartes–Sorbonne Paris Cité University, Imagine Institute, Paris, France

[7]CNRS ERL 8254, Paris, France

[8]Laboratory of Excellence GR-Ex, Paris, France

[9]Equipe Labélisée par la Ligue Nationale contre le cancer

[10]AB Science, Paris, France

[11]Department of Hematology, Necker Hospital, Paris, France

[12]Centre national de référence des mastocytoses (CEREMAST), Paris, France

[13]Linus Pauling Institute, Department of Biochemistry and Biophysics, Environmental Health Sciences Center, Oregon State University

Abstract

Distal axonopathy is a recognized pathological feature of amyotrophic lateral sclerosis (ALS). In the peripheral nerves of ALS patients, motor axon loss elicits a Wallerian-like degeneration

[j]**Corresponance to**:Luis Barbeito, Institut Pasteur de Montevideo, Mataojo 2020, Montevideo 11.400, Uruguay. (00598) 2 522 0910, barbeito@pateur.edu.uy.

[†]Deceased August 28th, 2019

Author contributions

ET, and LB designed the study. ET, MK, PHK, YS, YK, VV, and SI performed experiments. ET, PHK, YS, ICM, OH, JSB, and LB analyzed data. ET, PHK, ICM, JSB, OH, and LB prepared the manuscript. All authors contributed to the discussion of the results and edited and approved the final version of the manuscript.

Conflict of interest statement

OH is a co-founder and shareholder of AB science. Others have no conflict of interest.

Data availability

The data that support the findings of this study are available from the corresponding author upon reasonable request.

characterized by denervated Schwann cells (SCs) together with immune cell infiltration. However, the pathogenic significance of denervated SCs accumulating following impaired axonal growth in ALS remains unclear. Here, we analyze SC phenotypes in sciatic nerves of ALS patients and paralytic SOD1^{G93A} rats, and identify remarkably similar and specific reactive SC phenotypes based on the pattern of S100b, GFAP, isolectin and/or p75^{NTR} immunoreactivity. Different subsets of reactive SCs expressed colony-stimulating factor–1 (CSF1) and Interleukin-34 (IL-34) and closely interacted with numerous endoneurial CSF-1R-expressing monocyte/macrophages, suggesting a paracrine mechanism of myeloid cell expansion and activation. SCs bearing phagocytic phenotypes as well as endoneurial macrophages expressed stem cell factor (SCF), a trophic factor that attracts and activates mast cells through the c-Kit receptor. Notably, a subpopulation of Ki67+ SCs expressed c-Kit in the sciatic nerves of SOD1^{G93A} rats, suggesting a signaling pathway that fuels SC proliferation in ALS. c-Kit+ mast cells were also abundant in the sciatic nerve from LS donors but not in controls. Pharmacological inhibition of CSF-1R and c-Kit with masitinib in SOD1^{G93A} rats potently reduced SC reactivity and immune cell infiltration in the sciatic nerve and ventral roots, suggesting a mechanism by which the drug ameliorates peripheral nerve pathology. These findings provide strong evidence for a previously unknown inflammatory mechanism triggered by SCs in ALS peripheral nerves that has broad application in developing novel therapies.

Graphical Abstract

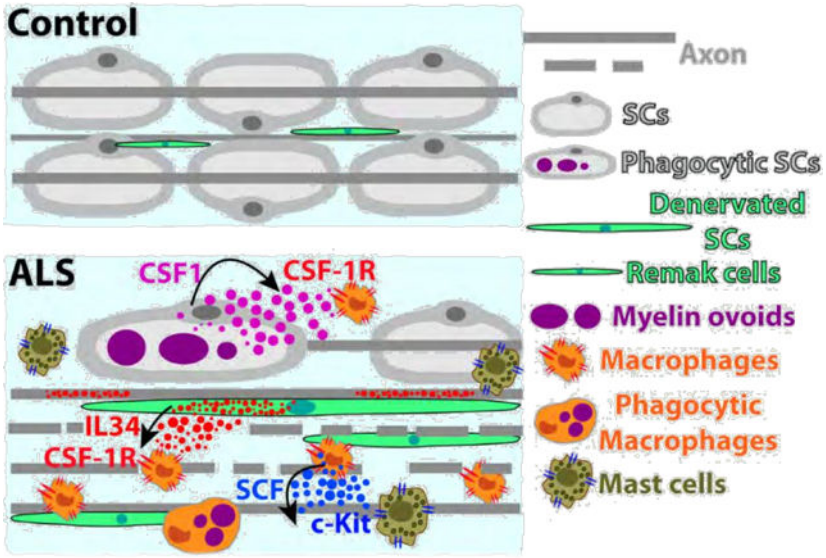

Keywords

Schwann cells; Peripheral nerve pathology; Inflammation; Tyrosine kinase receptors; Masitinib

Introduction

Distal motor axonopathy is one pathological feature of amyotrophic lateral sclerosis (ALS) that underlies the progressive skeletal muscle weakness and paralysis characteristic of the

disease (Fischer et al., 2004). Evidence in ALS patients and murine models expressing ALS-linked SOD1 mutations indicate that peripheral axons are lost before the death of cell bodies in the central nervous system (CNS) (Fischer et al., 2004; Frey et al., 2000; Kennel, Finiels, Revah, & Mallet, 1996). Degeneration of motor axons in ALS has been associated with defective axonal transport, mitochondria function and/or destabilization of neuromuscular junctions, among others (Arbour, Tremblay, Martineau, Julien, & Robitaille, 2015; Campanari, Garciayllon, Ciura, Saez- Valero, & Kabashi, 2016; Kong & Xu, 1998; Millecamps & Julien, 2013). The progressive loss of motor axons in ALS results in a Wallerian-like degeneration characterized by axon fragmentation, the disintegration of the axonal cytoskeleton, myelin degradation and immune cell infiltration (Chiu et al., 2009; Fischer & Glass, 2007), representing a stereotyped response to promote axonal growth and nerve repair. Following axonal loss, SCs become denervated and adopt an undifferentiated cell phenotype with profound transcriptional reprogramming and the upregulation of cytokines, chemokines and trophic factors (Jessen & Mirsky, 2016). In nerve injury, SCs can proliferate (Chang & Winkelstein, 2011), extend long processes across the gap to guide axonal growth (Gomez-Sanchez et al., 2017) or adopt phagocytic features to remove myelin (Brosius Lutz et al., 2017; Lindborg, Mack, & Zigmond, 2017). Unlike Wallerian degeneration, peripheral nerve pathology in ALS is not solely a reparative condition because the inexorable failure in effective axonal growth leads to a chronic and progressive degenerative and inflammatory condition. In this context, there is scarce knowledge about the specific phenotypes of SCs in ALS-associated degenerating peripheral nerves, in animal models or humans.

During Wallerian degeneration, a first step in the removal of myelin debris involves phagocytic SCs. This is followed by a second wave of phagocytic macrophages that are recruited by cytokines released by denervated SCs, such as LIF and MCP1 (Bigbee, Yoshino, & DeVries, 1987; Hirata & Kawabuchi, 2002; Stoll, Griffin, Li, & Trapp, 1989; Tofaris, Patterson, Jessen, & Mirsky, 2002). In turn, recruited macrophages become a source of secreted cytokine and trophic factor release, inducing a complex inflammatory cascade (Stratton et al., 2018; Tomlinson, Zygelyte, Grenier, Edwards, & Cheetham, 2018). Mast cells are also recruited (Esposito, De Santis, Monteforte, & Baccari, 2002), orchestrating complex vascular and immune cell responses, including the chemoattraction of phagocytic neutrophils that further contribute to myelin clearance (Lindborg et al., 2017). In comparison, ALS nerve pathology similarly involves reactive changes in SCs (Keller, Gravel, & Kriz, 2009) as well as the recruitment of monocytes, macrophages, mast cells and neutrophils (Chiu et al., 2009; Trias et al., 2018; Van Dyke et al., 2016).Such immune cell infiltration of the peripheral motor pathways in ALS has been linked to both protective and deleterious effects on motor neuron degeneration and disease progression (Nardo et al., 2016b). However, the functional link between SCs and immune cell influx to degenerating peripheral nerves in ALS remains unknown.

Of therapeutic interest in ALS, it has been demonstrated that downregulation of inflammation by tyrosine kinase inhibitor drugs such as GW2580 or masitinib is associated with decreased spinal nerve pathology and NMJ denervation, and prolonged survival in rodent models of ALS (Martinez-Muriana et al., 2016; Trias et al., 2016; Trias et al., 2018). In particular, masitinib has successfully completed a randomized, controlled, phase 2/3 trial

in ALS patients, showing a significant and clinically meaningful benefit for masitinib over placebo in relevant measures of disease progression (Mora et al., 2019). Thus, analysis of the cellular targets of masitinib in ALS peripheral nerve pathology may provide valuable information about disease mechanisms. Masitinib potently inhibits the ATPase subunit of CSF-1R and c-Kit receptors, both belonging to class III receptor tyrosine kinases (Anastassiadis, Deacon, Devarajan, Ma, & Peterson, 2011; Dubreuil et al., 2009). CSF-1R and c-Kit are typically expressed in myeloid cells and mast cells, respectively (Galli, Tsai, & Wershil, 1993; Stanley & Chitu, 2014). In SOD1^{G93A} rats developing paralysis, masitinib downregulates mast cells and neutrophil infiltration in both the sciatic nerve and skeletal muscle motor nerve terminals (Trias et al., 2017; Trias et al., 2018). In addition, masitinib decreases CSF-1R-dependent microgliosis in the lumbar spinal cord, suggesting a multitarget and multifaceted effect involving various inflammatory pathways in the central and peripheral nervous systems (Trias et al., 2016). However, there is little understanding of the specific cellular mechanisms that mediate the recruitment of CSF-1R- and c-Kit-expressing immune cells in the ALS peripheral nerve.

CSF1 and IL-34 are the two endogenous cognate ligands of CSF-1R, which upon activation stimulates monocyte/macrophage differentiation pattern and the acquisition of a phagocytic phenotype (Boulakirba et al., 2018). On the other hand, SCF is the ligand of c-Kit, which in peripheral tissues is mainly expressed in mast cells (Iemura, Tsai, Ando, Wershil, & Galli, 1994). SCF/c-Kit signaling drives chemoattraction of mast cell precursors, their differentiation into mature mast cells and ultimate degranulation, with the release of inflammatory and vasoactive molecules (Galli et al., 1993). Mast cells are key in orchestrating chronic inflammation and immune cell infiltration (Metz et al., 2007) and recently have been reported to extensively infiltrate the muscle and sciatic nerve of ALS patients and SOD1^{G93A} rats (Trias et al., 2017; Trias et al., 2018). The cellular sources of CSF1, IL-34, and SCF in ALS peripheral nerves remain largely unknown.

Here, we have analyzed the cellular localization of cytokines CSF1, IL-34 and SCF expressed in sciatic nerves of ALS patients and SOD1^{G93A} rats. We report for the first time, the upregulation of the three ligands in specific subsets of SCs, which are spatially associated with macrophages and mast cells expressing CSF-1R and c-Kit, respectively. Notably, a subset of proliferating SCs expressed c-Kit. Finally, systemic pharmacological inhibition of CSF-1R and c- Kit by masitinib sharply decreased SC reactivity, immune cell infiltration and proliferation along the peripheral motor pathways, providing evidence for an inflammatory mechanism triggered by SCs that can be therapeutically targeted in ALS.

Materials and Methods

Animals.

Male SOD1^{G93A} progeny were used for further breeding to maintain the line. Rats were housed in a centralized animal facility with a 12-h light-dark cycle with *ad libitum* access to food and water. Perfusion with fixative was performed under 90% ketamine – 10% xylazine anesthesia and all efforts were made to minimize animal suffering, discomfort or stress. All procedures using laboratory animals were performed in accordance with the national and international guidelines and were approved by the Institutional Animal Committee for

animal experimentation (CEUA Approved protocol: #005–17 to Dr. Luis Barbeito). This study was carried out in strict accordance with the Institut Pasteur de Montevideo Committee's requirements and under the current ethical regulations of the Uruguayan Law N° 18.611 for animal experimentation that follow the Guide for the Care and Use of Laboratory Animals of the National Institutes of Health (USA).

Experimental conditions.

At least 5 rats were analyzed for each experiment. Four different conditions were studied as follow: 1) non-transgenic (NonTg) rats of 160–180 days; 2) transgenic $SOD1^{G93A}$ rats of 180–190 days (symptomatic, onset); 3) transgenic $SOD1^{G93A}$ rats of 195–210 days treated with vehicle (paralysis, 15d-vehicle) and 4) transgenic $SOD1^{G93A}$ rats of 195–210 days treated with 30 mg/kg/d of masitinib during 15 days (paralysis, 15d-masitinib).

Determination of disease onset.

All rats were weighed and evaluated for motor activity daily as described (Trias et al., 2016; Trias et al., 2017). Disease onset was determined for each animal when pronounced muscle atrophy was accompanied by an abnormal gait, typically expressed as subtle limping or dragging of one hind limb.

Masitinib administration.

As described previously (Trias et al., 2017; Trias et al., 2018), only transgenic rats showing weakness and gait alterations in hind limbs as the first clinical sign were selected for masitinib treatment studies. Male rats were divided randomly into the masitinib or vehicle-treated groups. Masitinib mesylate (AB1010), freshly prepared in drinking sterilized water, was administrated daily at a dose of 30 mg/kg using a curved stainless steel gavage needle with 3-mm ball tip. Dosing was defined in accordance to previous studies in the same rat model of ALS that was shown to be safe for chronic treatments (Trias et al., 2016; Trias et al., 2017). Rats were treated from day-1 post-paralysis for an additional 15 days, when they were then euthanized.

Sciatic nerve and ventral roots cryopreserved sections.

Paraformaldehyde (4%) fixed sciatic nerve and ventral roots were cryopreserved in 30% sucrose (Sigma) at 4 °C. The 72 hours preserved sciatic nerve was embedded in TissueTek (Sakura), sectioned (longitudinal and transverse) at 10 μm using a cryostat, and collected on gelatin-coated slides.

Immunohistochemistry of $SOD1^{G93A}$ rat sciatic nerve and ventral root slices.

Longitudinal sciatic nerve sections and cross sections of ventral roots were blocked for 2 h at room temperature (5% BSA, 0.5% Triton X-100 in PBS), incubated with primary antibodies overnight at 4°C in 1% BSA, 0.3%Triton X- 100 in PBS. Antibodies used were: 1:250 rat polyclonal anti-c-Kit-biotin (abcam, #ab25022), 1:200 mouse anti-Tryptase (abcam, #ab134932), 1:300 mouse-anti Chymase (abcam, #ab111239), 1:200 mouse monoclonal anti-CD11b (BD Bioscience, #BD550299), 1:200 rabbit polyclonal anti-CSF-1R (Santa Cruz Biotechnology, #sc-692), 1:200 mouse monoclonal anti-CSF-1R (Santa

Cruz Biotechnology, #sc-46662), 1:250 mouse monoclonal anti-CD68 (abcam, #ab31630), 1:300 Isolectin-Biotin probe (Thermo Fisher Scientific, #I21414), 1:400 mouse monoclonal anti-GFAP (Sigma, #G3893), 1:400 rabbit polyclonal anti-GFAP (Sigma, #G9269), 1:300 mouse monoclonal anti-S100b (Sigma, #S2532), 1:300 mouse monoclonal anti-neurofilament200-AlexaFluor555 (Thermo Fisher Scientific, #MAB5256A5), 1:200 rabbit polyclonal anti-IL34 (Santa Cruz Biotechnology, #sc-135176), 1:250 rabbit polyclonal anti-CSF1 (Thermo Fisher Scientific, #PA5–42558), 1:300 Myelin-AlexaFluor488 or AlexaFluor546 probes (Thermo Fisher Scientific, #F34652), 1:250 rabbit polyclonal SCF (Thermo Fisher Scientific, #PA5–20746), 1:250 rabbit polyclonal anti-$p75^{NTR}$ (abcam #ab8874), 1:300 mouse monoclonal anti-S100 (Dako, Z0311), 1:200 rabbit polyclonal anti-Iba1 (Wako, #019–19741), 1:300 rabbit polyclonal anti-Ki67 (abcam, #ab16667). After incubation with primary antibodies, slices were washed with PBS 3 times for 10 min, incubated with secondary antibodies for 2 h at room temperature, 1:500 goat anti-rabbit-AlexaFluor488 (Thermo Fisher Scientific, #A21052), 1:500 goat anti-mouse-AlexaFluor546 (Thermo Fisher Scientific, #A11035), 1:500 goat anti-mouse-AlexaFluor633 (Thermo Fisher Scientific, #A21052), 1:500 Streptavidin- AlexaFluor405 or AlexaFluor633 (Thermo Fisher Scientific, #S21375), washed with PBS 3 times for 5 min, and mounted in DPX mounting medium (igma). The specificity of CSF1, IL-34, and SCF antibodies was determined by performing antibody preincubation with CSF1, IL-34 and SCF proteins (ProsPec, #CYT-856, # CYT-863, and #CYT-323 respectively) at a 1:5 ratio antibody/ligand concentration (Supplementary Figure 2).

Histochemistry quantitative analysis.

For cytokines density analysis, CSF1, IL-34, and SCF density analysis were measured using ImageJ as previously described (Trias et al., 2018). At least 20 sections per sciatic nerve per animal (n=4) were analyzed. The number of CSF-1R, CD11b, CD68+, Iba1+, c-Kit+ and Ki67+ cells infiltrating the sciatic nerve and ventral roots of $SOD1^{G93A}$ rats were counted in 25x and 63x (for ventral roots) magnification confocal images using the ImageJ software. At least twenty confocal stacks (320 × 320 × 10 μm in Z) from four animals among conditions were analyzed. For Schwann cell density analysis in the ventral roots, GFAP/S100b density analysis was measured using ImageJ as previously described (Trias et al., 2018).

Human tissue collection.

The collection of postmortem human ALS and control samples was approved by the University of Alabama, Birmingham (UAB) Institutional Review Board. (Approved IRB Protocol: X091222037 to Dr. Peter H. King) All ALS patients were cared for at UAB and so detailed clinical records were available. Control samples were age-matched and were harvested from patients who expired from non-neurological causes. The average collection time after death was less than 10 hours. All tissues were harvested by PHK and YS at the time of autopsy and preserved within 30 minutes. Control sciatic nerve tissues were obtained from the National Disease Research Interchange (NDRI).

Human sciatic nerve and ventral root immunohistochemistry.

Sciatic nerve and ventral root paraffin sections were sliced (10 μm) using a microtome. Following deparaffinization, slices were blocked and permeabilized in 5% BSA / 0.5%

Triton X-100 for 2 hours at room temperature. Primary antibodies were incubated in 1% BSA/0.5% Triton X-100 at 4°C overnight. Primary antibodies used were described. After washing, secondary antibodies were incubated for 3 hours at room temperature. After PBS washing, Mowiol medium (Sigma-Aldrich) was used for mounting.

Toluidine blue staining of the human sciatic nerve.

For the mast cell analysis based in metachromasia observation, as previously described (Trias et al., 2018), 10 μm sections of paraffin-embed human sciatic nerves were microtome sliced and mounted in positive-charged slides. Slides were deparaffinized before starting staining. Sections were washed and hydrated 2 times in distilled water for 10 minutes and embedded in 1% toluidine blue solution for 20 minutes. Then, slides were washed in distilled water 3 times 5 minutes and dehydrated during 3 minutes in 70 % ethanol, 3 minutes in 95 % ethanol and finally 2 minutes in 100 % ethanol. Slides were cleared in xylene twice, 3 minutes each and finally mounted in DPX (Sigma). 10x, 20x and 100x images were acquired using an Olympus CX41 microscope connected to a EvolutionTMLC Color camera and using ImagePro Express software for acquisition.

Real-time PCR analysis of the proximal sciatic nerve.

At least 4 proximal sections of sciatic nerve were dissected from NonTg and SOD1^{G93A} symptomatic rats. Tissue was processed for each mRNA extraction using Trizol Reagent (Thermo Fisher) and the aqueous phase was further purified using the RNeasy Mini kit (QIAGEN) according to the manufacturer's instructions. mRNA yields were measured on Nanodrop device (Thermo Scientific) and cDNA were obtained from 0.5 μg of RNA (−80 °C), 4 μL of iScript reverse transcription Supermix for RT-qPCR (BIORAD, −20 °C) in a final volume of 20 μL filled with nuclease free water. The Thermo cycler was set as follows: priming 5 min at 25 °C followed by 20 min at 46 °C for reverse transcription and 1 min at 95 °C for RT inactivation. RT-qPCR was performed on reverse transcribed cDNA using SsoAdvanced™ Universal SYBR® Green Supermix (BIO-RAD) on a Step One Plus Real-Time PCR System. For each well, 2 μL of diluted DNA was added to 8 μL of mix (containing 1 μL of each primer, 5 μL of SsoAdvanced™ Universal SYBR® Green Supermix, 1 μL of nuclease free water). Each sample was run in triplicate. The cycling parameters were as follows: 10 min at 95 °C then 40 cycles at 95 °C for 15 s and 1 min at 60 °C. Cq values were obtained for every cycle. Primers were designed on NCBI Primer-BLAST following the best guidelines to exclude genomic DNA amplification. The analysis was done using StepOne Software. Variations between samples were normalized using hypoxanthine-guanine phosphoribosyl transferase (HPRT) as a housekeeping gene. All primers were validated for specificity and efficiency. Primers used are:

CS1-Fw: 5´-AAAGTTTGCCT GGTGCTCTC-3´ CSF1-Rv: 5´-TTCGTTCGCTTCCTTGCTCG-3´. IL- 34-Fw:5´-TCTTGCTGCAAACAAAGTCCC-3' IL-34- Rv: 5ÁCACGTTGGTAGCTGCACAT-3´. SCF-Fw: 5´-TCCTCTCGTCAAAACTCAGGA-3´ SCF-Rv: 5´- CGGCGACATAGTTGAGGGTT-3´. HPRT-Fw: 5´- GTCATGTCGACCCTCAGTCC-3´ HPRT-Rv: 5´-GCAAGTCTTTCAGTCCTGTCC-3´.

Western Blot analysis

For protein extraction, proximal sciatic nerves from 4 non-transgenic and 4 symptomatic animals were dissected and homogenized in lysis buffer (50 mM HEPES pH 7.5, 50 mM NaCl, 1% Triton X-100, and complete protease inhibitor mixture (Roche, #11873580001), and then sonicated 3 times for 3 sec. Protein concentration was measured with a Bicinchoninic Acid (BCA) kit (Sigma, #QPBCA). Then, protein extracts were placed in loading buffer containing 15% SDS, 0.3 M Tris pH 6.8, 25% Glycerol, 1.5 M β-mercaptoethanol and 0.01% Bromphenol Blue. Protein samples (30 μg) were resolved on 12% SDS- polyacrylamide gel and transferred to PVDF membrane (Thermo, #88518). Membranes were blocked for 1h in Tris-buffered saline (TBS), 0.1% Tween-20 and 5% BSA, followed by overnight incubation at 4°C with the correspondent primary antibody diluted in the same buffer. Primary antibodies used in this study were rabbit anti-CSF1 (Thermo Fisher Scientific, #PA5–42558) and rabbit anti-IL34 (MBS, #2001373). After washing with 0.1% Tween in TBS, membranes were incubated with peroxidase-conjugated secondary antibody, goat anti-rabbit IgG to (Abcam, #ab6721) for 1 h, washed and developed using the SuperSignal West Pico Chemiluminiescent Substrate (Thermo Fisher Scientific, #34080). aActin was used as housekeeping. For aActin membranes were stripped according to the Mild Stripping protocol from bcam and then were incubated with mouse anti-aActin antibody (SIG A #A5441). After washing with 0.1% Tween in TBS, the membranes were incubated with secondary antibody, goat anti-mouse IgG (Abcam, #ab6728), and developed. All antibodies were used at dilutions recommended by the manufacturers. The images were obtained with Syngene GBox-Chemi 16 Bio Imaging System and densitometry was analyzed using ImageJ.

Fluorescence Imaging.

Fluorescence imaging was performed with a laser scanning Zeiss LSM 800 or LSM 880 confocal microscope with either a 25x (1.2 numerical aperture) objective or 63x (1.3 numerical aperture) oil-immersion objective using Zeiss Zen Black software. Maximum intensity projections of optical sections were created with Zeiss Zen software. Maximum intensity projections of optical sections, as well as 3D reconstructions, were created with Zeiss Zen software.

Statistics analysis.

Quantitative data were expressed as mean ± SEM. Two-tailed Mann-Whitney test or Kruskal-Wallis followed by Dunn’s multiple comparison test were used for statistical analysis, with $p<0.05$ considered significant. GraphPad Prism 7.03 software was used for statistical analyses.

Results

Characterization of Schwann cells in the ALS degenerating sciatic nerve

Previous studies on ALS postmortem peripheral nerve pathology have provided scarce information on SC phenotypes (Nardo et al., 2016a; Riva et al., 2016). We examined SCs by immunohistochemical analysis of 3 nerve specimens from ALS subjects and 3 control

donors, as well as one ALS ventral root specimen. Table 1 shows the characteristics of ALS patients and control subjects.

In longitudinal and transversal sections of the sciatic nerves from control donors, SCs were identified by S100b immunohistochemistry, with typical staining restricted to Schmidt-Lanterman clefts (Figure 1a–b). GFAP staining was low or absent in sections from control nerves. In contrast, all ALS specimens displayed a robust increase in both GFAP and S100b staining (Figure 1c–d), suggesting a significant SC reactivity. In longitudinal sections, GFAP staining labeled elongated SCs with a morphology resembling denervated or repair non-myelinating SCs (Figure 1c). S100b labeled a different subset of SCs, the morphology of which resembled myelinating or re- myelinating SCs (Figure 1c, lower panel). These SC phenotypes are similar to those observed in Wallerian degeneration (Gomez-Sanchez et al., 2017). A similar pattern of differential GFAP and S100b staining in SC subsets was observed in sciatic nerve sections from two other ALS patients and in one ventral root specimen (Figure 1d–e).

Understanding how specific SC phenotypes develop during active motor axon degeneration in $SOD1^{G93A}$ rats may allow a better understanding of nerve pathology in ALS. Sciatic nerves from non-transgenic control rats showed low GFAP expression in a few non-myelinating SCs and the typical S100b staining of myelinating SCs restricted to Schmidt-Lanterman clefts (Figure 2a), the morphology being closely similar to human control cases. Also, the $SOD1^{G93A}$ rat sciatic nerve analyzed either at hind limb paralysis onset or advanced paralysis, largely reproduced the SCs pathology observed in ALS subjects, with a robust upregulation of S100b and the appearance of a variety of SC phenotypes expressing GFAP (Figure 2a). As depicted in Figure 2b, SCs bearing S100b+ and GFAP+ represent two different cell populations corresponding to myelinating and denervated SCs, respectively. Denervated SCs were also identified by isolectin immunoreactivity, and myelin-laden SCs by S100 and $p75^{NTR}$ immunoreactivity (Figure 2b).

Schwann cells express of CSF1 and IL-34 in the ALS sciatic nerve

Previous reports have shown the expression of CSF1 in damaged peripheral nerve tissue associated with local recruitment of macrophages (Groh et al., 2012). In ALS rodent models, drugs inhibiting CSF-1R therapeutically decreased monocyte/macrophage infiltration (Martinez-Muriana et al., 2016), suggesting that locally expressed CSF1 and IL-34 are cognate CSF-1R ligands. As shown in Figure 3a and 3e, CSF1 and IL-34 were barely expressed in nerves from non-transgenic rats. In comparison, $SOD1^{G93A}$ rats showed robust endoneurial expression of CSF1 and IL-34 at paralysis onset, which further increased by 5–6-fold at advanced paralysis (Figure 3b, 3f). Upregulation of CSF1 and IL-34 in the degenerating $SOD1^{G93A}$ rat sciatic nerves was further confirmed by RT-PCR and Western blot analysis (Figure 3c–d; 3g–h; Supplementary Figure 1).

CSF1 was mainly expressed by a subset of phagocytic SCs typically engulfing myelin debris and stained with S100, S100b or $p75^{NTR}$ (Figure 3i, Supplementary Figure 3). In comparison, IL-34 was mainly expressed in a subset of denervated SCs (GFAP+/Isolectin+) with the morphology of repair SCs (or Bungner cells), aligned on the apparent trajectory of degenerating axons (Figure 3j, Suppl. Figure 3). In symptomatic $SOD1^{G93A}$ rats, CSF1 and

IL-34 were also localized in a subset of axons co-localizing with neurofilament staining (Supplementary Figure 4).

In the sciatic nerves from ALS donors, CSF1 and IL-34 were upregulated in the endoneurium as compared with weak immunoreactivity in control subjects (Figure 3k). While, the exact cellular localization of CSF1 and IL-34 in postmortem tissues was not precise, in some ALS nerve specimens, CSF1 and IL-34 were localized in elongated SC-like cells.

Schwann cells spatially interact with CSF-1R+ monocytes/macrophages

In the degenerating sciatic nerves of $SOD1^{G93A}$ rats, SCs were typically surrounded by clusters of CSF-1R+ macrophages (Figure 4a). CSF-1R immunoreactivity sharply increased by 10- and 20-fold at onset and advanced paralysis, respectively, when compared to non-transgenic rats (Figure 4a and Supplementary Figure 5a). Most CSF-1R immunoreactivity was found in the surface of small myeloid cells expressing CD68 or CD11b (Figure 4b and Supplementary Figure 5b) but not in myelin-laden phagocytic CD68+ macrophages (Figure 4c), suggesting CSF-1R expression in newly infiltrating monocyte/macrophages cells but not in fully differentiated macrophages.

Next, we addressed whether SF-1R immune cells infiltrate the sciatic nerve of ALS patients. Figure 4d shows the immunostaining of CSF-1R and CD68 in one sciatic and one ventral root from ALS patients, compared with control donors. CSF-1R+ immune cells infiltrated the ALS tissue in both the sciatic nerve and the ventral root but not in control donors (Figure 4d).

SCF is expressed in phagocytic Schwann cells and endoneurial macrophages

We have previously reported that c-Kit+ mast cells significantly infiltrate the peripheral motor pathway in ALS rats (Trias et al., 2018), suggesting the presence of increased levels of the ligand SCF. As shown in Figure 5a, SCF was below the limit of detection in the sciatic nerves of non-transgenic rats. In contrast, SCF immunoreactivity was increased in the sciatic nerve of $SOD1^{G93A}$ rats at disease onset and further increased by 4-fold at advanced paralysis as compared with onset (Figure 5b). Similarly, mRNA levels for SCF were increased by ~2 fold in the sciatic nerve of SOD1G93A rats at paralysis stage respect to non-transgenic controls (Figure 5c)

SCF was localized in a minority subset of phagocytic SCs bearing myelin debris and displaying p75NTR staining (Figure 5d) and also in monocytes and macrophages labeled with CD11b or CD68, respectively (Figure 5e).

Figure 5f shows that SCF was expressed in Iba1+ macrophages that infiltrate into the sciatic nerve of ALS patients but not in control donors.

c-Kit is expressed in proliferating Schwann cells and mast cells

Signaling through c-Kit supports the proliferation of undifferentiated SCs in neurofibromatosis type-1 (Dang, Nelson, & DeVries, 2005), however, it is unknown whether non-neoplastic SCs can also express the receptor. Here, we explored whether SCF

upregulation in ALS sciatic nerve was associated with SC proliferation. Remarkably, c-Kit was expressed in a subset of denervated SCs stained with GFAP or Isolectin (Figure 6a) but not in non-transgenic rats (Figure 6a, inset). Some c-Kit+ S s also displayed immunoreactivity for the cell proliferation marker Ki67 (Figure 6b).

In accordance with our previous reports showing mast cell infiltration along the peripheral motor pathway of SOD1G93A rats (Trias et al., 2017; Trias et al., 2018), the c-Kit receptor was mostly expressed in mast cells infiltrating the ALS sciatic nerves. Figure 6c shows the spatial interaction between denervated SCs and c-Kit+ mast cells. Comparatively, c-Kit+ mast cells were increased in all sciatic nerve and ventral root specimens from ALS subjects, as compared with controls (Figure 6d–e and Supplementary Figure 6).

Pharmacological inhibition of CSF1-R and c-Kit prevents Schwann cell reactivity in degenerating ventral roots.

We have previously shown that sciatic nerve pathology in symptomatic SOD1G93A rats is reduced by post-paralysis treatment with masitinib (Trias et al. 2018), a drug inhibiting CSF1-R and c-Kit receptors. Here, we have found that lumbar ventral roots at SOD1G93A rat at advanced paralysis also displayed an increased number of reactive SCs expressing GFAP and S100b as compared with non-transgenic rats (Figure 7a). A 15-day treatment with masitinib (30 mg/Kg/day) starting overt paralysis onset resulted in a 57% and 44% decrease in GFAP and S100b immunoreactivity, respectively, as compared to vehicle (Figure 7b).

Masitinib reduces immune cell infiltration and cell proliferation in the sciatic nerve.

Next, we have explored whether masitinib also reduced the number of immune cells dependent of CSF-1R and c-Kit receptors as well as cell proliferation. As shown in Figure 8a–b the number of infiltrating C 68+/Iba1+ macrophages, and c-Kit+ mast cells sharply increased during the course of the disease, with respect to non-transgenic animals. Post-paralysis treatment with masitinib reduced the number of CD68+ and Iba1+ macrophages by 30 and 60%, respectively (Graph in Figure 7a) as well as c-Kit+ mast cells by 30% (Graph in Figure 7b). Moreover, the number of proliferating cells estimated by Ki67+ nuclei staining decreased by 5-fold in masitinib-treated $SOD1^{G93A}$ rats (Graph in Figure 7c). More than 80% of Ki67+ nuclei in the degenerating sciatic nerve were localized in small S100+ SCs, while only a small percent were localized other cell types including macrophages (Supplementary Figure 7).

Discussion

We identified specific SC phenotypes in ALS degenerating peripheral nerves with the potential to trigger local inflammation through the expression of ligands for CSF-1R and c-Kit. SCs in human and $SOD1^{G93A}$ rat ALS sciatic nerves displayed remarkably similar phenotypic features, suggesting a conserved and stereotyped glial response to motor axon degeneration. SCs are regarded as key players in repair following nerve injury through the upregulation of cytokines and trophic factors (Jessen & Arthur-Farraj, 2019; Jessen & Mirsky, 2016). SCs in ALS expressed significant levels of CSF1, IL-34, and SCF and spatially interacted with immune effector cells bearing CSF-1R and c-Kit, suggesting a

complex cellular interplay leading to local inflammation. Previous studies have shown infiltrating macrophages, mast cells and neutrophils (Chiu et al., 2009; Nardo et al., 2016b; Trias et al., 2018) as well as SC proliferation (Deng et al., 2018) in the sciatic nerve of rodent ALS models. Here, we identified that these immune effectors express CSF-1R and c-Kit in human ALS nerves. Therefore, SCs expressing CSF1, IL-34 and SCF become pathophysiologically and therapeutically relevant in ALS.

It is known that SCs follow a profound phenotypic remodeling after nerve injury allowing repair and axonal growth (Gomez-Sanchez et al., 2017; Jessen & Arthur-Farraj, 2019). n ALS-affected nerves from patients with advanced paralysis and several years of disease progression, we found a comparable reactivity of SCs together with immune cell infiltration, suggesting SCs chronically retain pro-inflammatory features. Thus, the common perception of SCs as pathogenically passive cells in ALS peripheral nerves should be revised in view of their ability to orchestrate local inflammation in advanced stages of the disease. By comparing SCs in the sciatic nerve of sporadic ALS subjects and rats bearing the $SOD1^{G93A}$ mutation, we found similar SC phenotypes and inflammatory effectors, suggesting SC response to denervation is not greatly influenced by SOD1 mutations. Our study has not analyzed whether the expression of cytokines by SCs in ALS is influenced by the simultaneous expression of mutant SOD1. Of note, the reduction of mutant SOD1 levels within SCs in $SOD1^{G37R}$ mice significantly accelerates the paralysis progression (Lobsiger et al., 2009), suggesting mutant SOD1 could promote a protective activity in SCs.

Increased levels of CSF1 in peripheral nerves have been implicated in Charcot–Marie-Tooth disease type 1 neuropathy, where CSF1 appears to be expressed in endoneurial fibroblasts (Groh et al., 2015). In the ALS degenerating sciatic nerve, we found that CSF1 was mainly expressed in S100+/S100b+/$p75^{NTR}$+phagocytic SCs containing myelin debris, suggesting a mechanism inducing CSF1 expression in SCs and indirectly promoting monocyte/macrophage recruitment. However, because non-myelinating reactive SCs display fibroblast-like features (Ma et al., 2018), it can not be excluded that endoneurial fibroblasts also express CSF1 in ALS degenerating nerves. In comparison, IL-34 was strongly expressed in a different subset of GFAP+/Isolectin+, non- phagocytic reactive SCs, indicating that CSF1 and IL-34 expression is differently regulated in SCs phenotypes.

As far as we know, IL-34 expression in SCs has not been previously described. Because this cytokine does not solely activate CSF-1R but also exert local immunomodulatory function through the activation of PTP**z** receptors, it remains to be determined whether IL-34 exerts local immunoregulation on macrophages (Nandi et al., 2013). Thus, while CSF1 and IL-34 are CSF-1R ligands, the production of these cytokines by different subsets of SCs may be a key pathway underlying endoneurial monocyte/macrophage accumulation and their subsequent local protective or pathogenic effects.

While accumulation of macrophages has been previously described in the degenerating nerves of ALS subjects and murine models (Chiu et al., 2009; Kano, Beers, Henkel, & Appel, 2012; Kerkhoff et al., 1993), there is conflicting evidence as to whether macrophage infiltration is deleterious or rather protective in ALS (Nardo et al., 2016b). We found that the number of endoneurial myeloid cells closely correlates with axon loss and paralysis

progression in SOD1^{G93A} rats, suggesting a pathogenic role. This is in agreement with previous reports showing that pharmacological blockade of macrophages through CSF-1R inhibition is neuroprotective in the sciatic nerve of SOD1^{G93A} mice (Martinez-Muriana et al., 2016; Trias et al., 2018) as well as in a mouse models of Charcot-Marie-Tooth type 1 neuropathies (Klein et al., 2015). Thus, SCs could orchestrate focal nerve inflammation by expressing CSF1 and IL-34 in ALS, through the recruitment of a specific subset of 'disease amplifier' macrophages (Klein & Martini, 2016).

The finding that CSF1 and IL-34 are also expressed in peripheral axons suggests that damaged neurons in ALS express and anterogradely transport the cytokines. Neurons are an important source of IL-34 and CSF1 (Greter et al., 2012; Wang et al., 2012) and CSF1 has a recognized trophic activity in several types of neurons (Chitu, Gokhan, Nandi, Mehler, & Stanley, 2016; Luo et al., 2013). In addition, CSF1 is induced in motor neurons following peripheral nerve lesions and mediates microglia expansion in the spinal cord (Guan et al., 2016; Okubo et al., 2016). Thus, the upregulation of CSF1 and IL-34 in the ALS sciatic nerve could have protective roles, stimulating axon growth or sprouting during nascent stages of the disease but deleterious effects during active nerve degeneration.

Previously, we have reported a significant infiltration of mast cells, macrophages and neutrophils along the degenerating motor axons in sciatic nerves and skeletal muscle (Trias et al., 2017; Trias et al., 2018). Here, we show that c-Kit-expressing mast cells also accumulate in the endoneurium of post-mortem sciatic nerve from ALS donors. Because mast cells crosstalk with macrophages and neutrophils, amplifying the inflammatory and cytotoxic potential (De Filippo et al., 2013), our data further support a complex cellular mechanism leading to focal neuropathy in ALS. We also found that SCF was progressively upregulated in the ALS degenerating sciatic nerve during paralysis progression, being mainly expressed by phagocytic SCs and infiltrating macrophages. Thus, SCF appears as a novel cytokine expressed by SCs in ALS, with the potential to promote mast cell differentiation, proliferation and degranulation (Ito et al., 2012). c-Kit+ mast cells are abundant in neurofibromatosis type-1 where SCF is produced by tumorigenic SCs carrying the *Nf1*$^{-/-}$ mutation (Staser, Yang, & Clapp, 2010), suggesting a role for SCF in mediating tumor growth and nerve tissue remodeling. Remarkably, we also identified a subset of proliferating SCs expressing the c-Kit receptor in the SOD1^{G93A} rat sciatic nerve, suggesting SCF/c-Kit signaling also regulates SC expansion.

The therapeutic use of tyrosine kinase inhibitor drugs targeting CSF-1R and c- Kit in neurodegenerative diseases has gained increasing attention in the past years as an alternative mechanism to downregulate central and peripheral nervous system inflammation (Klein et al., 2015; Martinez-Muriana et al., 2016; Olmos-Alonso et al., 2016; Trias et al., 2016; Trias et al., 2017). Two drugs of this class have been shown to prevent sciatic nerve pathology and prolong survival in ALS rodent models (Martinez-Muriana et al., 2016; Trias et al., 2016; Trias et al., 2018). In particular, masitinib is in an advanced stage of clinical development and has demonstrated significant treatment-effect in a prospectively defined subpopulation of ALS patients (Mora et al., 2019). In this context, the present study shows evidence that masitinib protection along the degenerating ALS ventral roots and sciatic nerves is mediated, at least in part, by inhibition of CSF-1R- and c-Kit-mediated inflammation. In addition,

masitinib ameliorated the increased cell proliferation observed in SOD1^{G93A} rats' sciatic nerves. Because S100+ cells bearing non-myelinating SCs morphology appear to account for 80% of dividing cells in degenerating nerves, these cells appear to be significant targets for masitinib.

In conclusion, the present study shows further evidence for the role of SCs orchestrating inflammation along the peripheral motor pathway in sporadic ALS subjects and SOD1^{G93A} rats. Although CSF1, IL-34, and SCF are expressed by specific subsets of SCs, the coordinated upregulation of the three cytokines suggests that they act in concert to trigger a complex cellular response, as summarized in Figure 9. The resulting accumulation of CSF-1R+ and c-Kit+ immune cells into ALS-affected ventral roots and peripheral nerves may become deleterious, leading to the development of secondary neuropathic lesions. In turn, healthy motor and sensory axons as well as intact myelinating SCs could be damaged, further accelerating motor neuron peripheral axonopathy and disease progression. Pharmacological inhibition by masitinib of deleterious inflammatory nerve damage, may further explain the multifaceted therapeutic effects of masitinib in ALS patients and animal models.

Supplementary Material

Refer to Web version on PubMed Central for supplementary material.

Acknowledgments

We want to thank Colin Mansfield for his critical comments and helpful suggestions revising the manuscript and the staff from the Transgenic and Experimental Animal Unit from Institut Pasteur de Montevideo. We are very grateful to our ALS patients who donated their tissues post-mortem to advance ALS research. We also thank the National Disease Research Interchange (NDRI) who provide control tissue. This work was supported by Institut Pasteur de Montevideo – FOCEM Mercosur (COF 03/11), the Amyotrophic Lateral Sclerosis Association (00482), Agencia Nacional de Investigación e Innovación (ANII), NINDS R01NS092651 (to PHK), Merit Review BX001148 from the Department of Veterans Affairs (to PHK), Programa de Desarrollo de las Ciencias Básicas (PEDECIBA), Sistema Nacional de Investigadores (SNI) and the Comisión Sectorial de Investigación Científica (CSIC), Universidad de la República, Uruguay; Grupos I+D Program, #1104.

References

Anastassiadis T, Deacon SW, Devarajan K, Ma H, & Peterson JR (2011). Comprehensive assay of kinase catalytic activity reveals features of kinase inhibitor selectivity. Nat Biotechnol, 29(11), 1039–1045. doi:10.1038/nbt.2017 [PubMed: 22037377]

Arbour D, Tremblay E, Martineau E, Julien JP, & Robitaille R. (2015). Early and persistent abnormal decoding by glial cells at the neuromuscular junction in an ALS model. J Neurosci, 35(2), 688–706. doi:10.1523/JNEUROSCI.1379-14.2015 [PubMed: 25589763]

Bigbee JW, Yoshino JE, & DeVries GH (1987). Morphological and proliferative responses of cultured Schwann cells following rapid phagocytosis of a myelin- enriched fraction. J Neurocytol, 16(4), 487–496. [PubMed: 3681350]

Boulakirba S, Pfeifer A, Mhaidly R, Obba S, Goulard M, Schmitt T, … Jacquel A. (2018). IL-34 and CSF-1 display an equivalent macrophage differentiation ability but a different polarization potential. Sci Rep, 8(1), 256. doi:10.1038/s41598-017-18433-4 [PubMed: 29321503]

Brosius Lutz A, Chung WS, Sloan SA, Carson GA, Zhou L, Lovelett E, … Barres BA (2017). Schwann cells use TAM receptor-mediated phagocytosis in addition to autophagy to clear myelin in a mouse model of nerve injury. Proc Natl Acad Sci U S A, 114(38), E8072–E8080. doi:10.1073/pnas.1710566114

Campanari ML, Garcia-Ayllon MS, Ciura S, Saez-Valero J, & Kabashi E. (2016). Neuromuscular Junction Impairment in Amyotrophic Lateral Sclerosis: Reassessing the Role of Acetylcholinesterase. Front Mol Neurosci, 9, 160. doi:10.3389/fnmol.2016.00160

Chang YW, & Winkelstein BA (2011). Schwann cell proliferation and macrophage infiltration are evident at day 14 after painful cervical nerve root compression in the rat. J Neurotrauma, 28(12), 2429–2438. doi:10.1089/neu.2011.1918 [PubMed: 21787151]

Chitu V, Gokhan S, Nandi S, Mehler MF, & Stanley ER (2016). Emerging Roles for CSF-1 Receptor and its Ligands in the Nervous System. Trends Neurosci, 39(6), 378–393. doi:10.1016/j.tins.2016.03.005 [PubMed: 27083478]

Chiu IM, Phatnani H, Kuligowski M, Tapia JC, Carrasco MA, Zhang M, … Carroll, M. C. (2009). Activation of innate and humoral immunity in the peripheral nervous system of ALS transgenic mice. Proc Natl Acad Sci U S A, 106(49), 20960–20965. doi:10.1073/pnas.0911405106 [PubMed: 19933335]

Dang I, Nelson JK, & DeVries GH (2005). c-Kit receptor expression in normal human Schwann cells and Schwann cell lines derived from neurofibromatosis type 1 tumors. J Neurosci Res, 82(4), 465–471. doi:10.1002/jnr.20648 [PubMed: 16235251]

De ilippo K, Dudeck A, Hasenberg M, Nye E, van Rooijen N, Hartmann K, … Hogg N. (2013). Mast cell and macrophage chemokines CXCL1/CXCL2 control the early stage of neutrophil recruitment during tissue inflammation. Blood, 121(24), 4930–4937. doi:10.1182/blood-2013-02-486217 [PubMed: 23645836]

Deng B, Lv W, Duan W, Liu Y, Li Z, Ma Y, … Li, C. (2018). Progressive Degeneration and Inhibition of Peripheral Nerve Regeneration in the SOD1- G93A Mouse Model of Amyotrophic Lateral Sclerosis. Cell Physiol Biochem, 46(6), 2358–2372. doi:10.1159/000489627 [PubMed: 29742495]

Dubreuil P, Letard S, Ciufolini M, Gros L, Humbert M, Casteran N, … Hermine O. (2009). Masitinib (AB1010), a potent and selective tyrosine kinase inhibitor targeting KIT. PLoS One, 4(9), e7258. doi:10.1371/journal.pone.0007258 [PubMed: 19789626]

Esposito B, De Santis A, Monteforte R, & Baccari GC (2002). Mast cells in Wallerian degeneration: morphologic and ultrastructural changes. J Comp Neurol, 445(3), 199–210. [PubMed: 11920701]

Fischer LR, Culver DG, Tennant P, Davis AA, Wang M, Castellano-Sanchez A, … Glass JD (2004). Amyotrophic lateral sclerosis is a distal axonopathy: evidence in mice and man. Exp Neurol, 185(2), 232–240. [PubMed: 14736504]

Fischer LR, & Glass JD (2007). Axonal degeneration in motor neuron disease. Neurodegener Dis, 4(6), 431–442. doi:10.1159/000107704 [PubMed: 17934327]

Frey D, Schneider C, Xu L, Borg J, Spooren W, & Caroni P. (2000). Early and selective loss of neuromuscular synapse subtypes with low sprouting competence in motoneuron diseases. J Neurosci, 20(7), 2534–2542. [PubMed: 10729333]

Galli SJ, Tsai M, & Wershil BK (1993). The c-kit receptor, stem cell factor, and mast cells. What each is teaching us about the others. Am J Pathol, 142(4), 965–974. [PubMed: 7682764]

Gomez-Sanchez JA, Pilch KS, van der Lans M, Fazal SV, Benito C, Wagstaff LJ, … Jessen KR (2017). After Nerve Injury, Lineage Tracing Shows That Myelin and Remak Schwann Cells Elongate Extensively and Branch to Form Repair Schwann Cells, Which Shorten Radically on Remyelination. J Neurosci, 37(37), 9086–9099. doi:10.1523/JNEUROSCI.1453-17.2017 [PubMed: 28904214]

Greter M, Lelios I, Pelczar P, Hoeffel G, Price J, Leboeuf M, … Becher B. (2012). Stroma-derived interleukin-34 controls the development and maintenance of langerhans cells and the maintenance of microglia. Immunity, 37(6), 1050–1060. doi:10.1016/j.immuni.2012.11.001 [PubMed: 23177320]

Groh J, Klein I, Hollmann C, Wettmarshausen J, Klein D, & Martini R. (2015). CSF-1-activated macrophages are target-directed and essential mediators of Schwann cell dedifferentiation and dysfunction in Cx32-deficient mice. Glia, 63(6), 977–986. doi:10.1002/glia.22796 [PubMed: 25628221]

Groh J, Weis J, Zieger H, Stanley ER, Heuer H, & Martini R. (2012). Colony- stimulating factor-1 mediates macrophage-related neural damage in a model for Charcot-Marie-Tooth disease type 1X. Brain, 135(Pt 1), 88–104. doi:10.1093/brain/awr283 [PubMed: 22094537]

Guan Z, Kuhn JA, Wang X, Colquitt B, Solorzano C, Vaman S, … Basbaum AI (2016). Injured sensory neuron-derived CSF1 induces microglial proliferation and DAP12-dependent pain. Nat Neurosci, 19(1), 94–101. doi:10.1038/nn.4189 [PubMed: 26642091]

Hirata K, & Kawabuchi M. (2002). Myelin phagocytosis by macrophages and nonmacrophages during Wallerian degeneration. Microsc Res Tech, 57(6), 541–547. doi:10.1002/jemt.10108 [PubMed: 12112437]

Iemura A, Tsai M, Ando A, Wershil BK, & Galli SJ (1994). The c-kit ligand, stem cell factor, promotes mast cell survival by suppressing apoptosis. Am J Pathol, 144(2), 321–328. [PubMed: 7508684]

Ito T, Smrz D, Jung MY, Bandara G, Desai A, Smrzova S, … Gilfillan AM (2012). Stem cell factor programs the mast cell activation phenotype. J Immunol, 188(11), 5428–5437. doi:10.4049/jimmunol.1103366 [PubMed: 22529299]

Jessen KR, & Arthur-Farraj P. (2019). Repair Schwann cell update: Adaptive reprogramming, EMT, and stemness in regenerating nerves. Glia, 67(3), 421–437. doi:10.1002/glia.23532 [PubMed: 30632639]

Jessen KR, & Mirsky R. (2016). The repair Schwann cell and its function in regenerating nerves. J Physiol, 594(13), 3521–3531. doi:10.1113/JP270874 [PubMed: 26864683]

Kano O, Beers DR, Henkel JS, & Appel SH (2012). Peripheral nerve inflammation in ALS mice: cause or consequence. Neurology, 78(11), 833–835. doi:10.1212/WNL.0b013e318249f776 [PubMed: 22377817]

Keller AF, Gravel M, & Kriz J. (2009). Live imaging of amyotrophic lateral sclerosis pathogenesis: disease onset is characterized by marked induction of GFAP in Schwann cells. Glia, 57(10), 1130–1142. doi:10.1002/glia.20836 [PubMed: 19115383]

Kennel PF, Finiels F, Revah F, & Mallet J. (1996). Neuromuscular function impairment is not caused by motor neurone loss in FALS mice: an electromyographic study. Neuroreport, 7(8), 1427–1431. [PubMed: 8856691]

Kerkhoff H, Troost D, Louwerse ES, van Dijk M, Veldman H, & Jennekens FG (1993). Inflammatory cells in the peripheral nervous system in motor neuron disease. Acta Neuropathol, 85(5), 560–565. [PubMed: 8493864]

Klein D, & Martini R. (2016). Myelin and macrophages in the PNS: An intimate relationship in trauma and disease. Brain Res, 1641(Pt A), 130–138. doi:10.1016/j.brainres.2015.11.033 [PubMed: 26631844]

Klein D, Patzko A, Schreiber D, van Hauwermeiren A, Baier M, Groh J, … Martini R. (2015). Targeting the colony stimulating factor 1 receptor alleviates two forms of Charcot-Marie-Tooth disease in mice. Brain, 138(Pt 11), 3193–3205. doi:10.1093/brain/awv240 [PubMed: 26297559]

Kong J, & Xu Z. (1998). Massive mitochondrial degeneration in motor neurons triggers the onset of amyotrophic lateral sclerosis in mice expressing a mutant SOD1. J Neurosci, 18(9), 3241–3250. [PubMed: 9547233]

Lindborg JA, Mack M, & Zigmond RE (2017). Neutrophils Are Critical for Myelin Removal in a Peripheral Nerve Injury Model of Wallerian Degeneration. J Neurosci, 37(43), 10258–10277. doi:10.1523/JNEUROSCI.2085-17.2017

Lobsiger CS, Boillee S, McAlonis-Downes M, Khan AM, Feltri ML, Yamanaka K, & Cleveland DW (2009). Schwann cells expressing dismutase active mutant SOD1 unexpectedly slow disease progression in ALS mice. Proc Natl Acad Sci U S A, 106(11), 4465–4470. doi:10.1073/pnas.0813339106 [PubMed: 19251638]

Luo J, Elwood F, Britschgi M, Villeda S, Zhang H, Ding Z, … Wyss-Coray, T. (2013). Colony-stimulating factor 1 receptor (CSF1R) signaling in injured neurons facilitates protection and survival. J Exp Med, 210(1), 157–172. doi:10.1084/jem.20120412 [PubMed: 23296467]

Ma D, Wang B, Zawadzka M, Gonzalez G, Wu Z, Yu B, … Zhao, C. (2018). A Subpopulation of Foxj1-Expressing, Nonmyelinating Schwann Cells of the Peripheral ervous System Contribute to Schwann Cell Remyelination in the Central Nervous System. J Neurosci, 38(43), 9228–9239. doi:10.1523/JNEUROSCI.0585-18.2018 [PubMed: 30228229]

Martinez-Muriana A, Mancuso R, Francos-Quijorna I, Olmos-Alonso A, Osta R, Perry VH, … Lopez-Vales R. (2016). CSF1R blockade slows the progression of amyotrophic lateral sclerosis by

reducing microgliosis and invasion of macrophages into peripheral nerves. Sci Rep, 6, 25663. doi:10.1038/srep25663

Metz M, Grimbaldeston MA, Nakae S, Piliponsky AM, Tsai M, & Galli SJ (2007). Mast cells in the promotion and limitation of chronic inflammation. Immunol Rev, 217, 304–328. doi:10.1111/j.1600-065X.2007.00520.x [PubMed: 17498068]

Millecamps S, & Julien JP (2013). Axonal transport deficits and neurodegenerative diseases. Nat Rev Neurosci, 14(3), 161–176. doi:10.1038/nrn3380 [PubMed: 23361386]

Mora J, Genge A, Chio A, Estol CJ, Chaverri D, Hernandez M., … Group AS (2019). Masitinib as an Add-on Therapy to Riluzole in Patients with Amyotrophic Lateral Sclerosis: A Randomised Clinical Trial. Amyotrophic Lateral Sclerosis and Frontotemporal Degeneration. doi:10.1080/21678421.2019.1632346

Nandi S, Cioce M, Yeung YG, Nieves E, Tesfa L, Lin H, … Stanley ER (2013). Receptor-type protein-tyrosine phosphatase zeta is a functional receptor for interleukin-34. J Biol Chem, 288(30), 21972–21986. doi:10.1074/jbc.M112.442731

Nardo G, Trolese MC, de Vito G, Cecchi R, Riva N, Dina G, … Bendotti C. (2016a). Immune response in peripheral axons delays disease progression in SOD1(G93A) mice. J Neuroinflammation, 13(1), 261. doi:10.1186/s12974-016-0732-2 [PubMed: 27717377]

Nardo G, Trolese MC, de Vito G, Cecchi R, Riva N, Dina G, … Bendotti C. (2016b). Immune response in peripheral axons delays disease. J Neuroinflammation, 13(1), 261. doi:10.1186/s12974-016-0732-2 [PubMed: 27717377]

Okubo M, Yamanaka H, Kobayashi K, Dai Y, Kanda H, Yagi H, & Noguchi K. (2016). Macrophage-Colony Stimulating Factor Derived from Injured Primary Afferent Induces Proliferation of Spinal Microglia and Neuropathic Pain in Rats. PLoS One, 11(4), e0153375. doi:10.1371/journal.pone.0153375

Olmos-Alonso A, Schetters ST, Sri S, Askew K, Mancuso R, Vargas-Caballero M, … Gomez-Nicola D. (2016). Pharmacological targeting of CSF1R inhibits microglial proliferation and prevents the progression of Alzheimer's-like pathology. Brain, 139(Pt 3), 891–907. doi:10.1093/brain/awv379 [PubMed: 26747862]

Riva N, Clarelli F, Domi T, Cerri F, Gallia F, Trimarco A, … Quattrini A. (2016). Unraveling gene expression profiles in peripheral motor nerve from amyotrophic lateral sclerosis patients: insights into pathogenesis. Sci Rep, 6, 39297. doi:10.1038/srep39297 [PubMed: 27982123]

Stanley ER, & Chitu V. (2014). CSF-1 receptor signaling in myeloid cells. Cold Spring Harb Perspect Biol, 6(6). doi:10.1101/cshperspect.a021857

Staser K, Yang FC, & Clapp DW (2010). Mast cells and the neurofibroma microenvironment. Blood, 116(2), 157–164. doi:10.1182/blood-2009-09-242875 [PubMed: 20233971]

Stoll G, Griffin JW, Li CY, & Trapp BD (1989). Wallerian degeneration in the peripheral nervous system: participation of both Schwann cells and macrophages in myelin degradation. J Neurocytol, 18(5), 671–683. [PubMed: 2614485]

Stratton JA, Holmes A, Rosin NL, Sinha S, Vohra M, Burma NE, … Biernaskie J. (2018). Macrophages Regulate Schwann Cell Maturation after Nerve Injury. Cell Rep, 24(10), 2561–2572 e2566. doi:10.1016/j.celrep.2018.08.004

Tofaris GK, Patterson PH, Jessen KR, & Mirsky R. (2002). Denervated Schwann cells attract macrophages by secretion of leukemia inhibitory factor (LIF) and monocyte chemoattractant protein-1 in a process regulated by interleukin-6 and LIF. J Neurosci, 22(15), 6696–6703. doi:20026699 [PubMed: 12151548]

Tomlinson JE, Zygelyte E, Grenier JK, Edwards MG, & Cheetham J. (2018). Temporal changes in macrophage phenotype after peripheral nerve injury. J Neuroinflammation, 15(1), 185. doi:10.1186/s12974-018-1219-0 [PubMed: 29907154]

Trias E, Ibarburu S, Barreto-Nunez R, Babdor J, Maciel TT, Guillo M, … Barbeito L. (2016). Post-paralysis tyrosine kinase inhibition with masitinib abrogates neuroinflammation and slows disease progression in inherited amyotrophic lateral sclerosis. J Neuroinflammation, 13(1), 177. doi:10.1186/s12974-016-0620-9 [PubMed: 27400786]

Trias E, Ibarburu S, Barreto-Nunez R, Varela V, Moura IC, Dubreuil P, … Barbeito L. (2017). Evidence for mast cells contributing to neuromuscular pathology in an inherited model of ALS. JCI Insight, 2(20). doi:10.1172/jci.insight.95934

Trias E, King PH, Si Y, Kwon Y, Varela V, Ibarburu S, … Barbeito L. (2018). Mast cells and neutrophils mediate peripheral motor pathway degeneration in ALS. JCI Insight, 3(19). doi:10.1172/jci.insight.123249

Van Dyke JM, Smit-Oistad IM, Macrander C, Krakora D, Meyer MG, & Suzuki M. (2016). Macrophage-mediated inflammation and glial response in the skeletal muscle of a rat model of familial amyotrophic lateral sclerosis (ALS). Exp Neurol, 277, 275–282. doi:10.1016/j.expneurol.2016.01.008 [PubMed: 26775178]

Wang Y, Szretter KJ, Vermi W, Gilfillan S, Rossini C, Cella M, … Colonna, (2012). IL-34 is a tissue-restricted ligand of CSF1R required for the development of Langerhans cells and microglia. Nat Immunol, 13(8), 753–760. doi:10.1038/ni.2360 [PubMed: 22729249]

Manuscript main points:

- Schwann cells expressing CSF1, IL-34, and SCF accumulate in the sciatic nerves from ALS subjects.
- Schwann cells interact with myeloid and mast cells expressing CSF-1R and c-Kit receptors, respectively.
- Pharmacological inhibition of CSF-1R and c-Kit ameliorates sciatic nerve pathology.

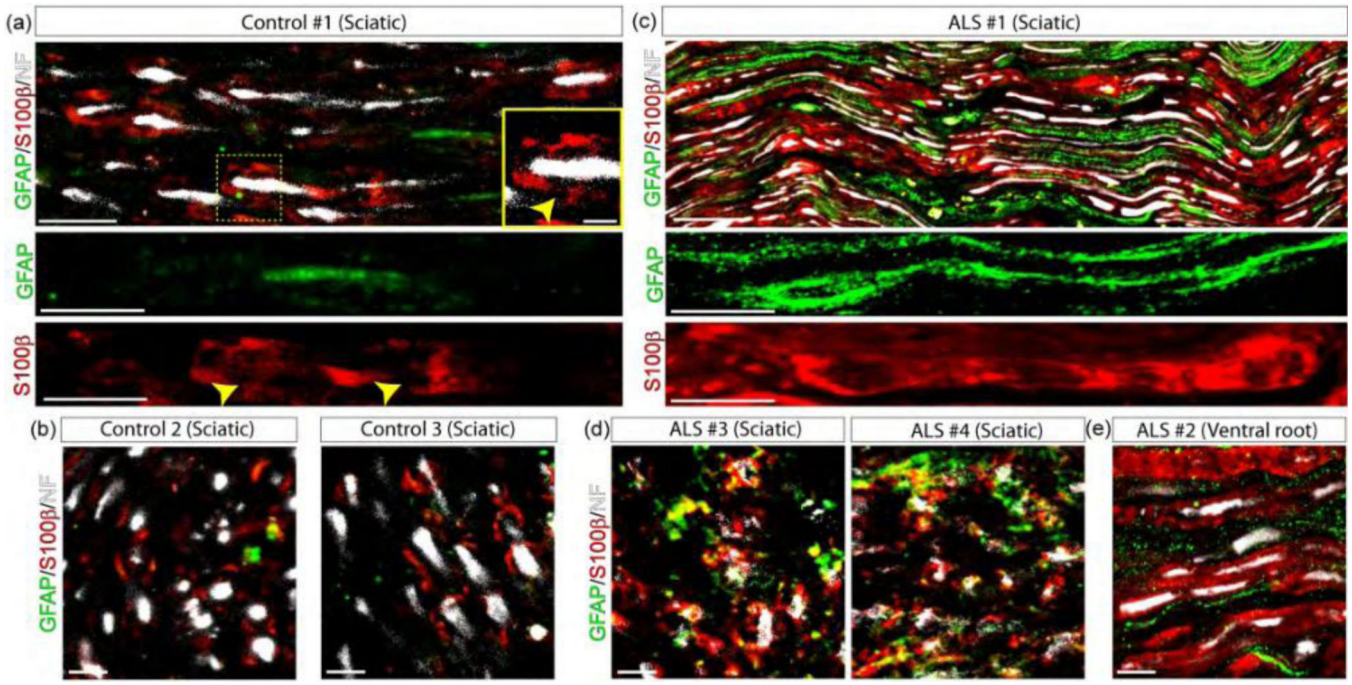

Figure 1.

SC phenotypes in the sciatic nerve of ALS patients. GFAP and S100β immunofluorescence confocal characterization of SCs in 10 μm sections of the sciatic nerve and one ventral root of ALS patients as compared with control donors. (a–b) 3 sciatic nerves from control donors were analyzed in longitudinal sections (upper panels) and cross-sections (lower panels). Note low GFAP expression, while S100β was restricted to Schmidt-Lanterman clefts (yellow arrowheads in inset). (c–d) 4 sciatic nerves from ALS patients were analyzed in longitudinal and cross-sections. Note GFAP and S100β increase in denervated and myelinating SCs, respectively, labeling different subsets of cells. (e) In comparison, GFAP and S100β were also expressed in different subsets of SCs in the ventral root from one ALS patient. Scale bars: 100 μm in and (c), 10 μm in (b), (d), and (e). 334×168mm (300 × 300 DPI)

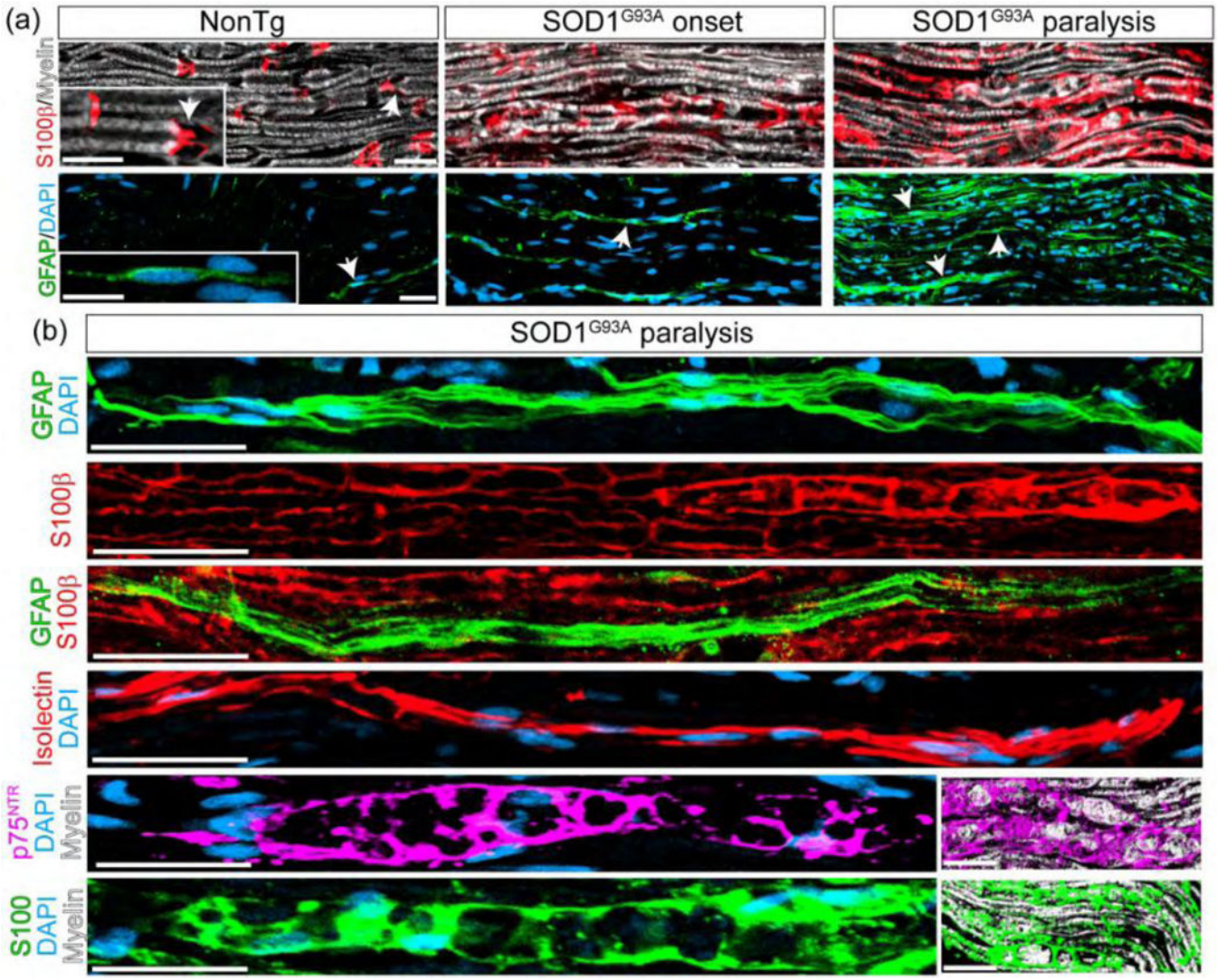

Figure 2.

SC phenotypes in the sciatic nerve of SOD1G93A rats during paralysis progression. Confocal immunostaining analysis of SC phenotypes in 10 μm sciatic nerve sections at onset and advanced paralysis as compared with non-transgenic littermates. (a) S100β and GFAP staining among conditions. Note S100β and GFAP expression restricted to Schmidt-Lanterman clefts (inset in the upper panel, white arrows) and Remak-like cells (arrow in the inset of lower panel), in NonTg rats, respectively, while both sharply increased during the course of the paralysis. (b) Confocal Immunophenotyping of SCs subpopulation in SOD1G93A symptomatic rats. Note that GFAP and Isolectin label denervated SCs, while S100, S100β and p75NTR label phagocytic or myelin-laden SCs (insets). Scale bars: 20 μm in (a) and 50 μm in (b). 178×142mm (300 × 300 DPI)

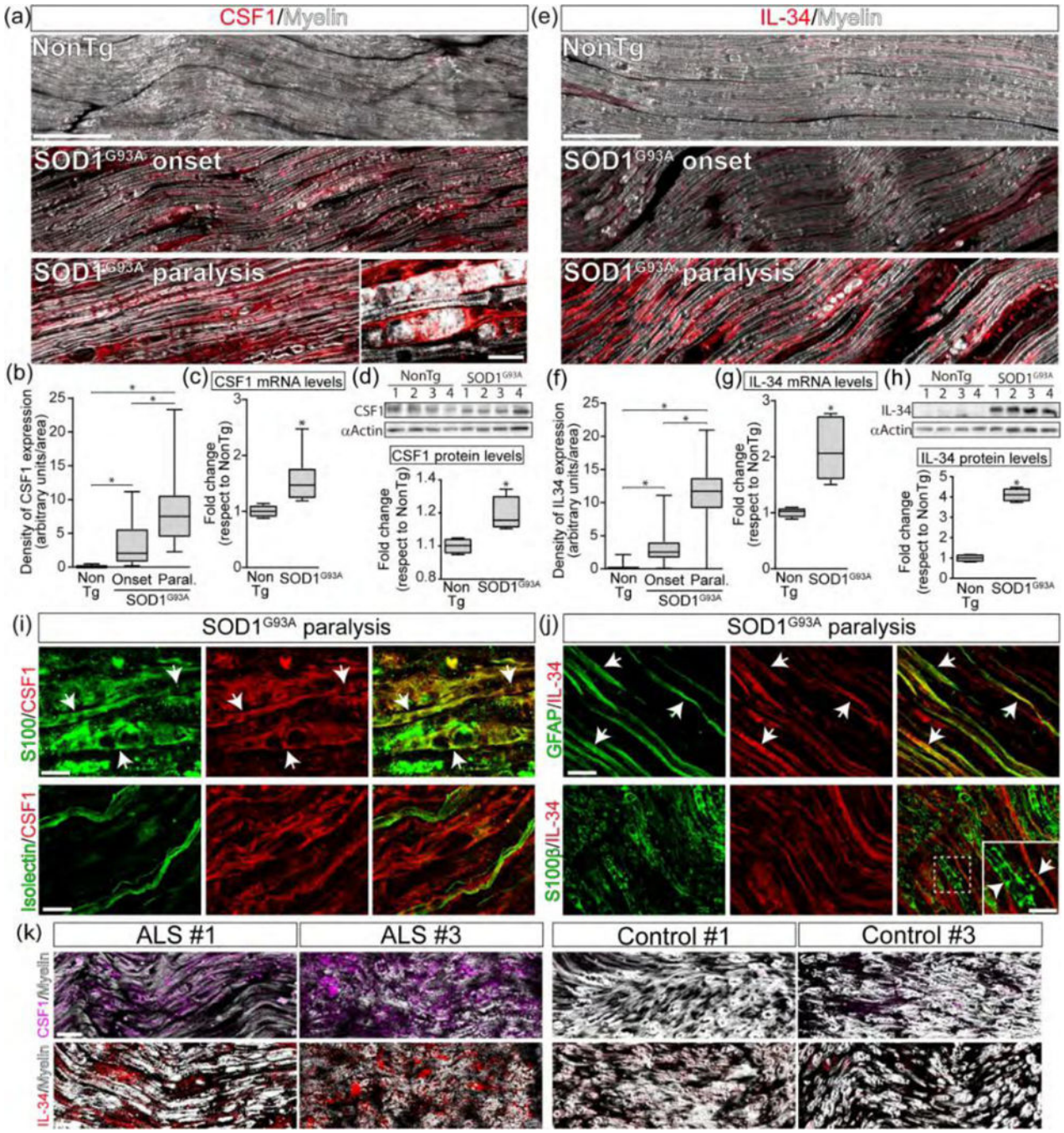

Figure 3.

SCs upregulate CSF1 and IL-34 in SOD1G93A sciatic nerve. (a) Immunohistochemical analysis of CSF1 expression in proximal sciatic nerve longitudinal sections during the course of the paralysis. Inset shows the characteristic phenotype of a phagocytic SCs expressing CSF1. (b) Quantitative analysis of the immunoreactivity for CSF1. (c, d) Analysis of mRNA and protein levels of CSF1 by RT-PCR and western blot in proximal sciatic nerves. The graph below shows western blot quantitative analysis. (e) Immunohistochemical analysis of Il-34 expression in proximal sciatic nerve longitudinal

sections during the course of the paralysis. (f) Quantitative analysis of the immunoreactivity for IL-34. (g, h) Analysis of mRNA and protein levels of IL- 34 by RT-PCR and western blot in proximal sciatic nerves. The graph below shows western blot quantitative analysis. (i, j) Identification of SCs expressing CSF1 (i) and IL-34 (j) in longitudinal sections of sciatic nerves during advanced paralysis in SOD1G93A rats. Note that CSF1 is mainly expressed in phagocytic S100+ SCs (white arrows) but not in denervated Isolectin+ SCs (lower panels), while IL-34 was mainly expressed in denervated GFAP+ SCs (white arrows). (k) Longitudinal sections of sciatic nerve showing the immunostaining analysis of CSF1 (magenta, upper panels) and IL-34 (red, lower panels) expression in ALS patients and controls. All data are expressed as mean ± SEM; data were analyzed by Kruskal-Wallis followed by Dunn's multiple comparison test (b, f) or Mann Whitney test (c, d, g,h), $p < 0.05$ was considered statistically significant. n=4/6 animals/condition. Scale bars: 100 μm in (a), 10 μm in (c) and (d). Scale bars: 100 μm in (a) and (e), 10 μm in (i) and (j), 25 μm in (k). 199×212mm (300 × 300 DPI)

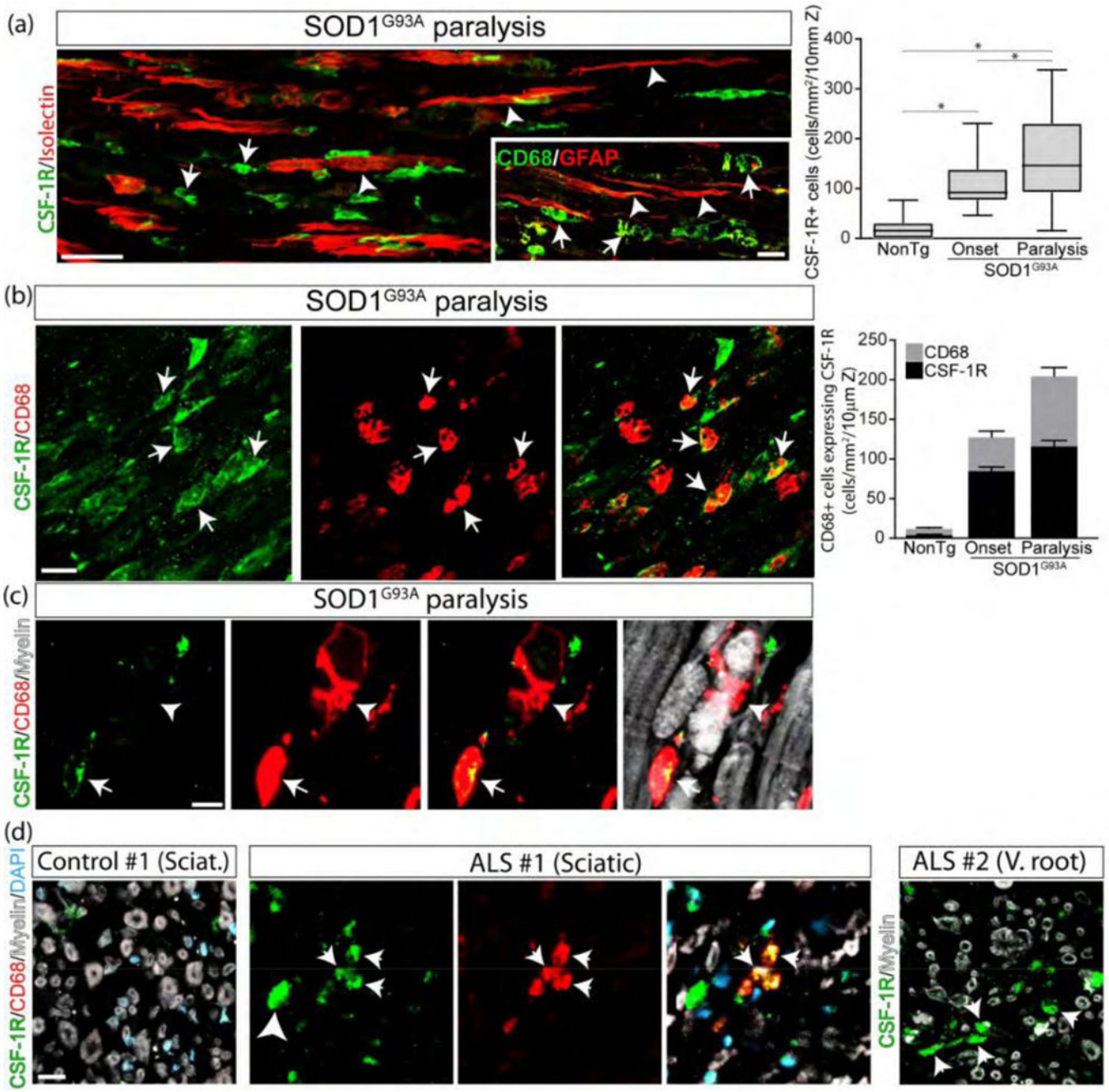

Figure 4.

SCs interact with CSF-1R+ macrophages. (a) Spatial association of denervated SCs expressing Isolectin or GFAP (white arrowheads) with CSF-1R+ and CD68+ macrophages (white arrows) in SOD1G93A rats and NonTg littermates. he graph to the right shows the quantitative analysis of CSF-1R+ cells into the sciatic nerve among conditions. (b) Identification of cells expressing CSF-1R. Note that CSF-1R+ cells mainly correspond to macrophages expressing CD68 (white arrows). The graph to the right shows the quantitative analysis of CD68+ macrophages expressing CSF-1R. (c) High magnification analysis showing a subset non-phagocytic C 68+ macrophages express CSF-1R (white arrow), while

phagocytic macrophages lose CSF-1R staining (white arrowhead). (d) CSF-1R expression analysis in cross-sections of the sciatic nerve and ventral root from ALS subjects. All quantitative data are expressed as mean ± SEM; data were analyzed by Kruskal-Wallis followed by Dunn's multiple comparison test. * indicates $p < 0.05$. n=4 animals/condition. Scale bars: 20 μm in (a), (b) and (d), and 10 μm in (c). 178×175mm (300 × 300 DPI)

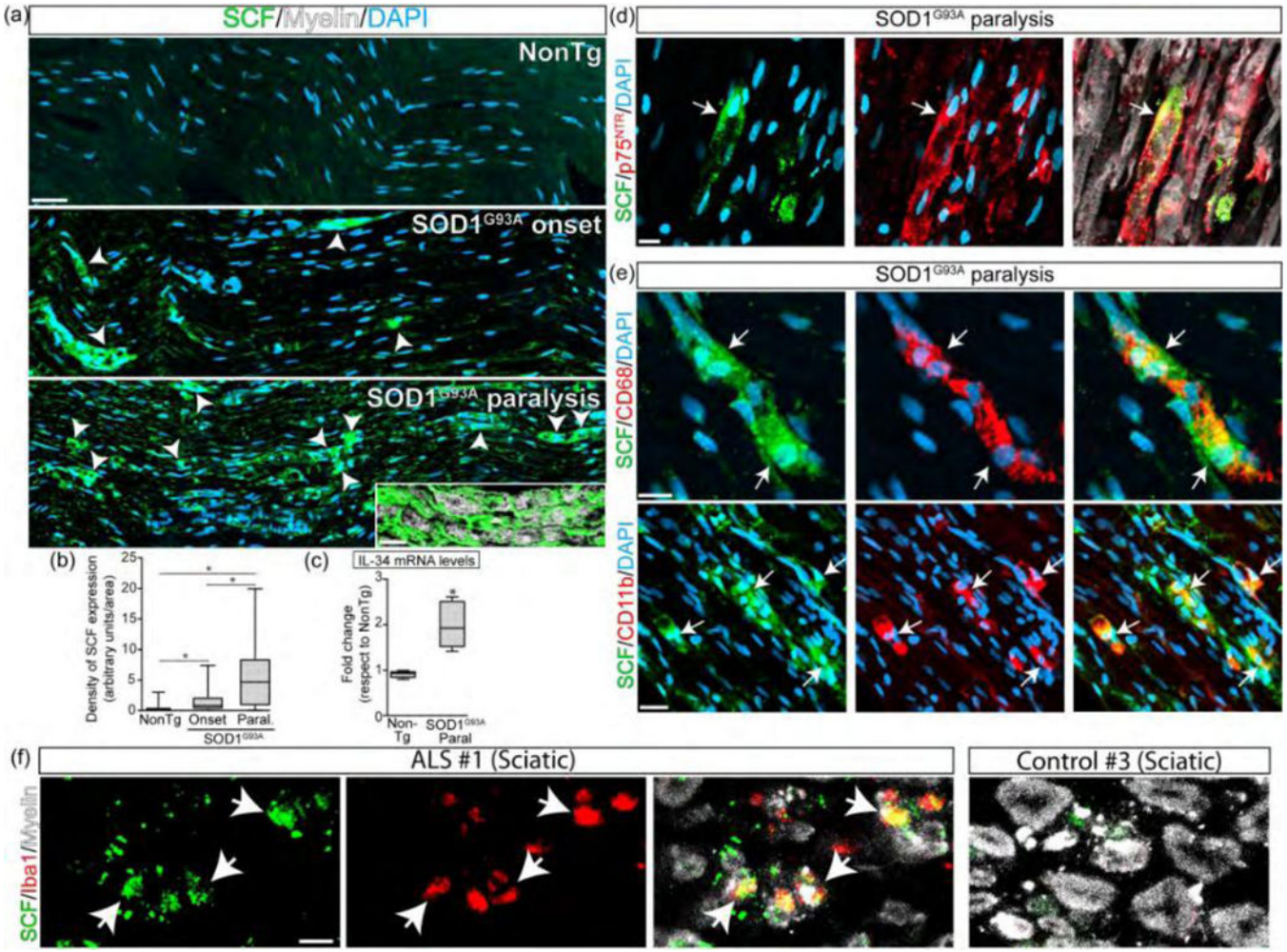

Figure 5.

SCs and macrophages express SCF in ALS sciatic nerve. (a) Immunohistochemical analysis of SCF expression in longitudinal sections during the course of the paralysis in SOD1G93A rats. Note the sharp increase of the cytokine in phagocytic S s in symptomatic rats (white arrowheads and inset). (b) Quantitative analysis of SCF expression among groups. (c) Analysis of mRNA levels of SCF by RT-PCR. (d) Confocal images showing the expression of SCF in SCs. Note that SCF is expressed by reactive p75NTR+ SCs (white arrow). (e) Confocal images showing the SCF expression in macrophages. Note that SCF is also expressed by CD68+/CD11b+ cells (white arrows). (f) SCF expression analysis in cross-sections sciatic nerves from ALS subjects. ll data are expressed as mean ± SEM; data were analyzed by Kruskal- Wallis followed by Dunn's multiple comparison test (b) or Mann Whitney test (c), $p < 0.05$ was considered statistically significant. n=4/6 animals/condition. Scale bars: 50 μm in (a), 20 μm in inset (a), 10 μm in (c) and (d), and 10 μm in (e). 255×189mm (300 × 300 DPI)

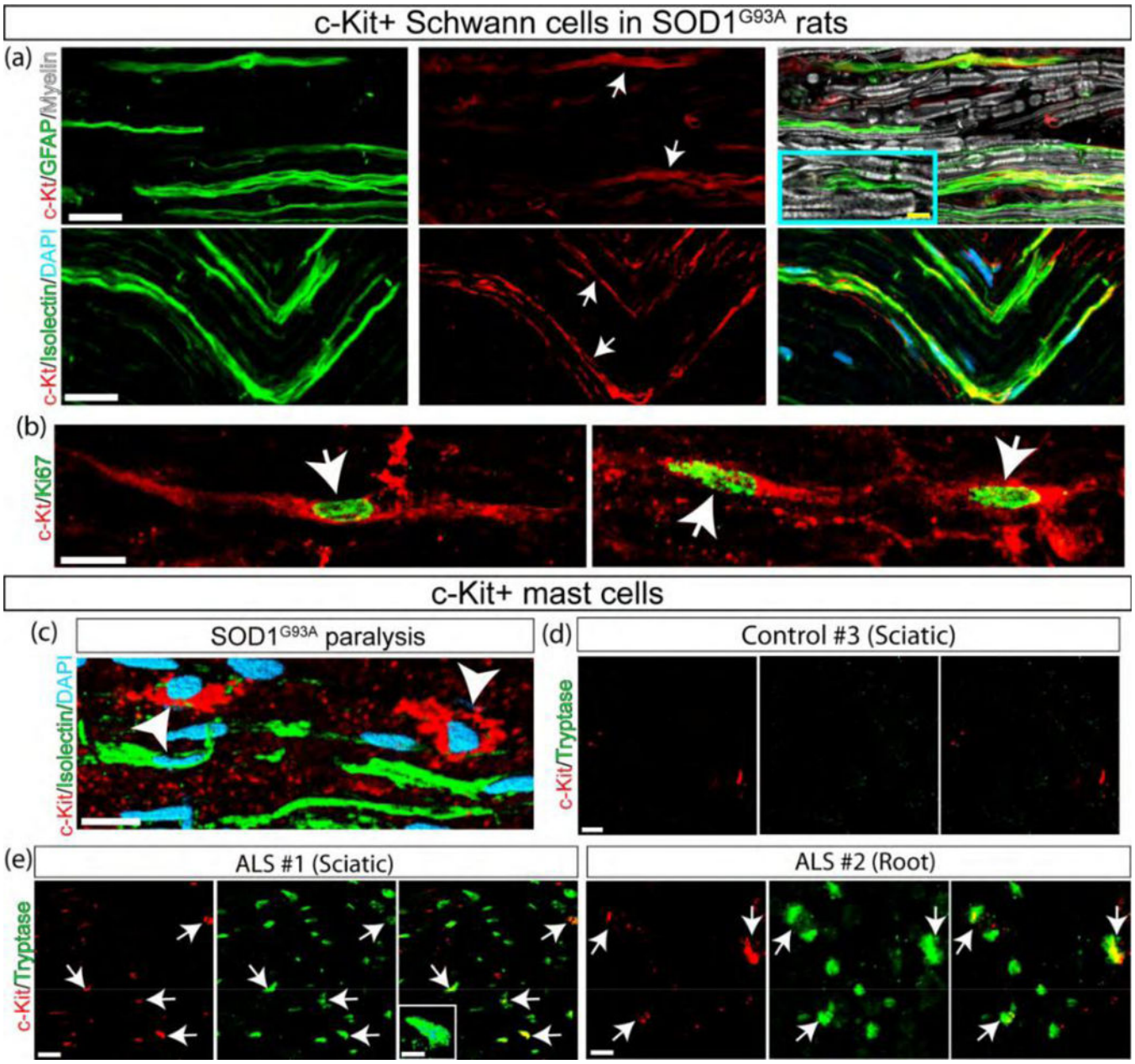

Figure 6.

Proliferating SCs and mast cells express c-Kit in the ALS sciatic nerve. (a) Longitudinal sections of SOD1G93A sciatic nerve during advanced paralysis showing c-Kit expression in denervated GFAP+/Isolectin+ SCs (white arrows). Inset shows GFAP+ SCs in NonTg rats. (b) A subpopulation of c- Kit+ SCs expresses the proliferation marker Ki67 (white arrows). (c) c-Kit is also expressed in endoneurial mast cells (white arrowhead). (d, e) Confocal images showing c-Kit+ mast cells infiltrating into the human ALS sciatic nerve. Note that c-Kit+ or Tryptase+ cells were not detected in sciatic nerve cross-sections from controls (d), while endoneurial c-Kit+/Tryptase+ mast cells accumulate in the sciatic nerve and ventral root from ALS cases (white arrows in e). Dotted lines represent the border of myelin sheaths. Scale bars: 10 μm in (a–c) and 5 μm in (e). 171×160mm (300 × 300 DPI)

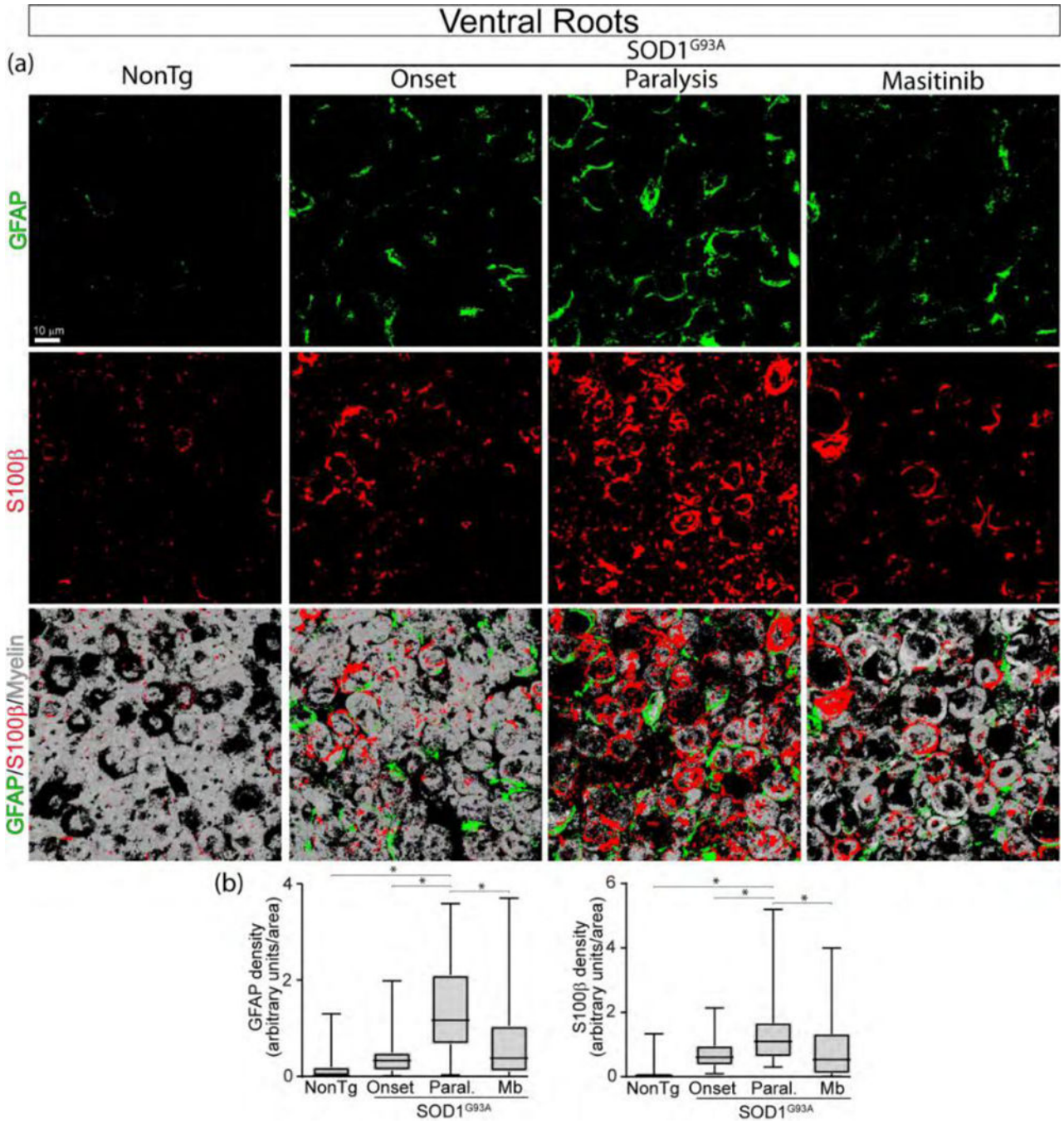

Figure 7.

Masitinib prevents SC reactivity in degenerating ventral roots of SOD1G93A rats. Masitinib (30 mg/kg/day) was orally administered for 15 days starting after paralysis onset. (a) Representative 3D confocal images of ventral root cross-sections showing SCs stained for GFAP (green) and S100β (red). Note that few SCs were observed in NonTg rats, but reactive SCs accumulated during disease progression. Masitinib treatment significantly prevented SC reactivity and improved ventral root pathology estimated by myelin staining (white). Scale bar: 10 μm. (b) Graphs show the quantitative analysis of the density of SCs per area. All

quantitative data are expressed as mean ± SEM; data were analyzed by Kruskal-Wallis followed by Dunn's multiple comparison test, $p < 0.05$ was considered statistically significant. n=4 animals/condition. 167×176mm (300 × 300 DPI)

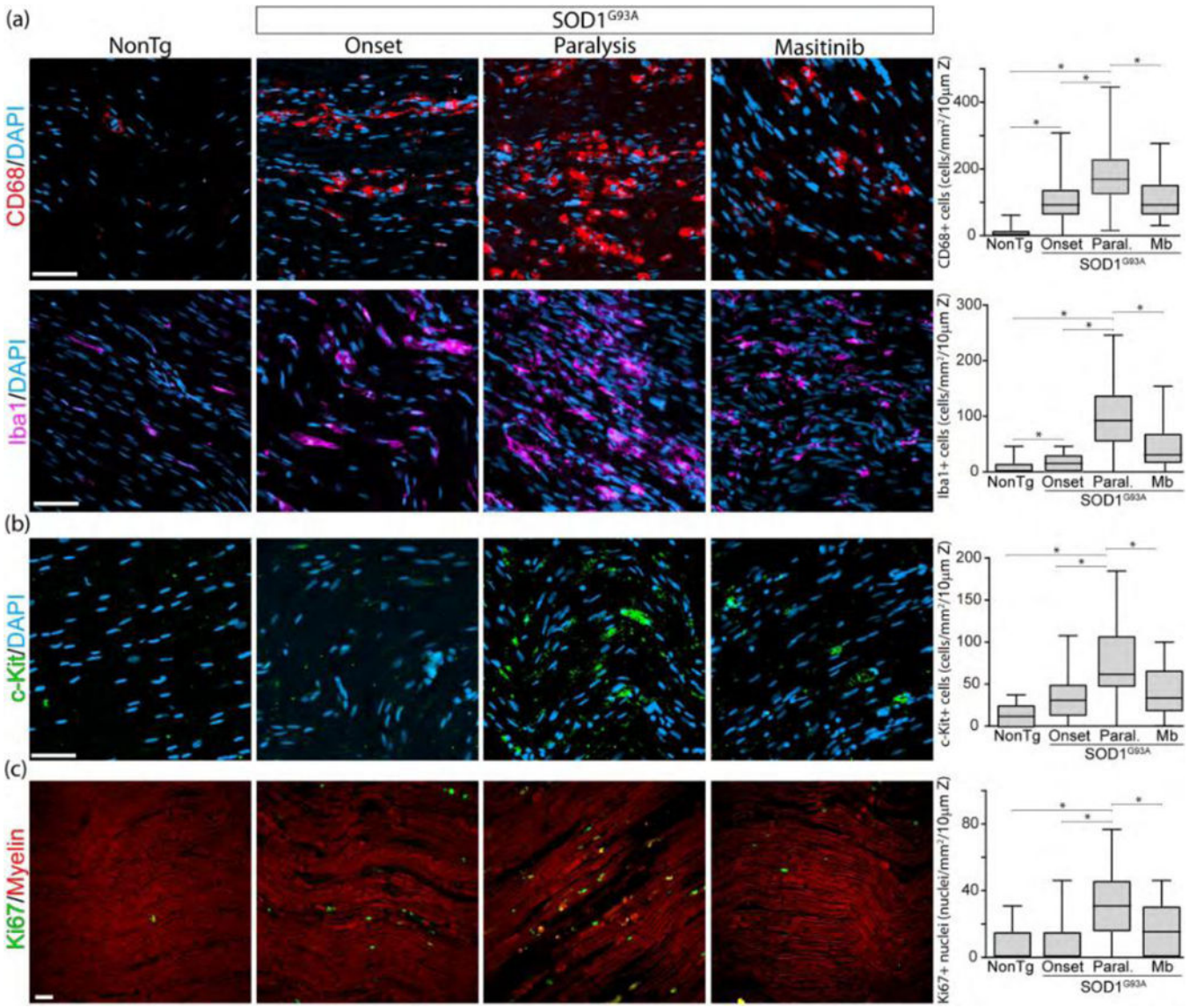

Figure 8.

Masitinib reduces immune cell infiltration and proliferation. Immunohistochemical analysis of immune cell infiltration and cell proliferation in the sciatic nerve among conditions. Rats were treated as described in Figure 7. (a, b) Confocal images show the increasing accumulation of CD68+ and Iba1+ macrophages, and c-Kit+ mast cells during the course of the paralysis, as compared with non-transgenic littermates. In all cases, masitinib treatment significantly reduced immune cell infiltration. Graphs to the right show the quantitative analysis of the respective immune cell types among conditions. (c) Analysis of cell proliferation in the sciatic nerve assessed by Ki67 immunostaining. The graph to the right shows Ki67 quantitative analysis. All quantitative data are expressed as mean ± SEM; data were analyzed by Kruskal-Wallis followed by Dunn's multiple comparison test, * indicates $p < 0.05$. n=4 animals/condition. Scale bars: 20 µm in (a)–(c). 213×180mm (300 × 300 DPI)

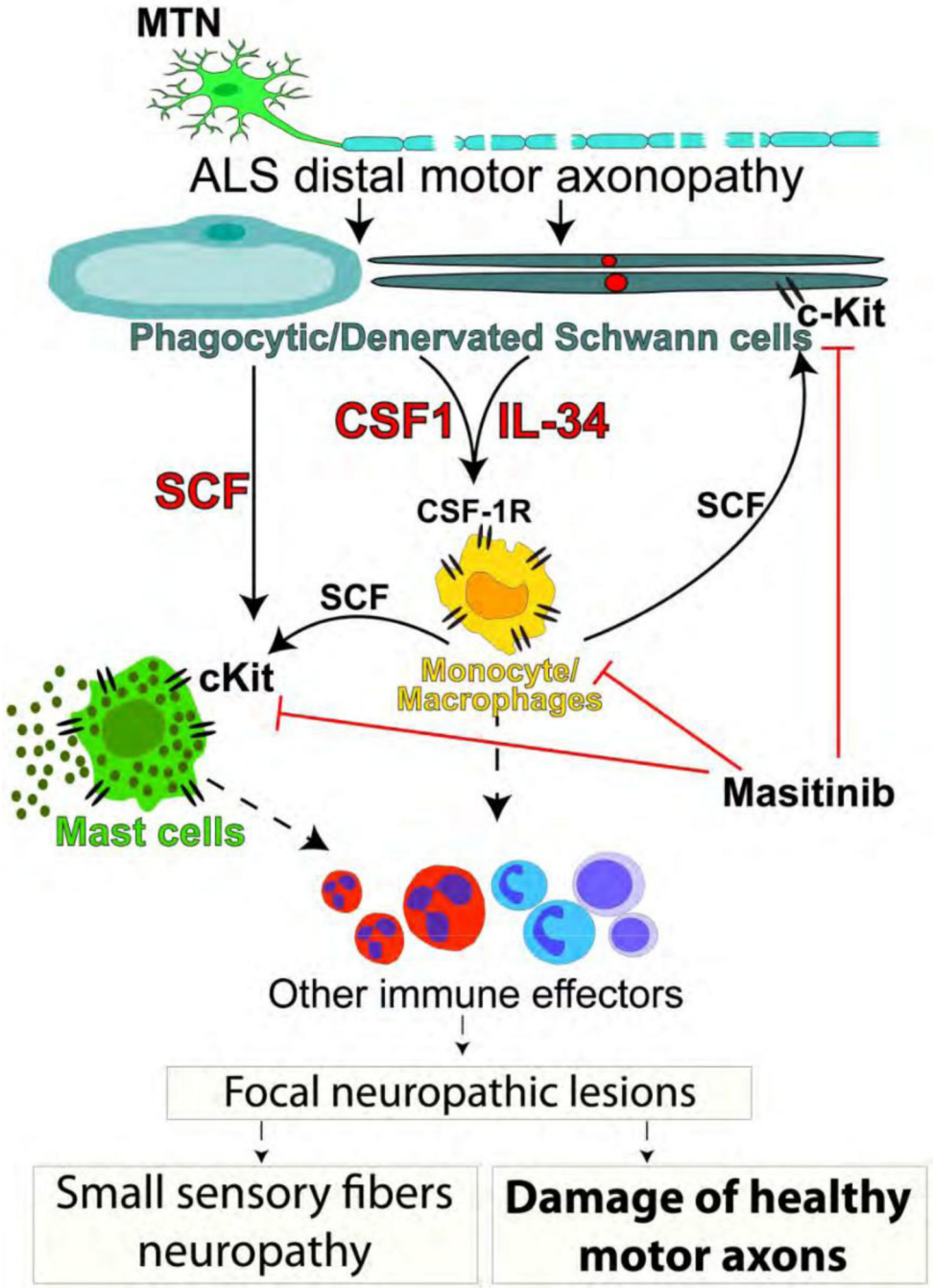

Figure 9.

Schematic hypothesis about the pathogenic role of SCs in ALS. Reactive SCs expressing CSF1, IL-34 and SCF accumulate in ALS peripheral nerves as a consequence of primary motor axon pathology. These cytokines trigger monocytes/macrophages and mast cell influx and activation through CSF-1R and c-Kit, which in turn, stimulate a complex inflammatory response involving other immune cell effectors, leading to focal neuropathic lesions with the potential to induce damage of adjacent healthy motor axons and sensory fibers.

Pharmacological inhibition of CSF-1R and c-Kit may reduce the inflammatory load.
204×283mm (300 × 300 DPI)

Table 1:

Clinical characteristics of ALS and control subjects included in the study.

Subject	Age* (years)	Gender	Disease onset	Survival** (Months)	Cause of death
ALS #1	69	F	Leg	52	-
ALS #2	40	M	Arm	63	-
ALS #3	76	M	Bulbar	32	-
ALS #4	75	M	Leg	58	-
Control #1	64	M	-	-	Cardiac
Control #2	79	M	-	-	Cardiac
Control #3	74	F	-	-	Stroke

*Age of death.

**From onset to death.